CHAPTER FIVE

Mechanisms Underlying Anomalous Diffusion in the Plasma Membrane

Diego Krapf
Department of Electrical and Computer Engineering and School of Biomedical Engineering, Colorado State University, Fort Collins, CO, USA
E-mail: krapf@engr.colostate.edu

Contents

Current Topics in Membranes, Volume 75
ISSN 1063-5823
http://dx.doi.org/10.1016/bs.ctm.2015.03.002

Abstract

The plasma membrane is a complex fluid where lipids and proteins undergo diffusive motion critical to biochemical reactions. Through quantitative imaging analyses such as single-particle tracking, it is observed that diffusion in the cell membrane is usually anomalous in the sense that the mean squared displacement is not linear with time. This chapter describes the different models that are employed to describe anomalous diffusion, paying special attention to the experimental evidence that supports these models in the plasma membrane. We review models based on anticorrelated displacements, such as fractional Brownian motion and obstructed diffusion, and nonstationary models such as continuous time random walks. We also emphasize evidence for the formation of distinct compartments that transiently form on the cell surface. Finally, we overview heterogeneous diffusion processes in the plasma membrane, which have recently attracted considerable interest.

1. INTRODUCTION

The plasma membrane separates the interior of the cell from the outside world maintaining intracellular components inside a living cell. As the interface between the cell and the extracellular fluid, the plasma membrane is responsible for a myriad of functions essential for cell physiology. These functions include the uptake of nutrients, such as sugars or amino acids, the regulation of ionic intracellular concentrations via the combination of transporters and channels, and the delivery of materials to the extracellular space (exocytosis). One of the most important functions of the cell membrane is the initiation of complex signaling cascades by recognizing and internalizing small molecules, which enable cell communication. Signaling pathways through the plasma membrane also control metabolism, growth and differentiation of tissues, and synthesis of proteins (Alberts et al., 2010; Lodish et al., 2007).

Given that the cell membrane is fluid, signaling reactions therein are limited by the rate at which reactants find each other. Thus, reactions are governed by the diffusive transport of membrane components. One would expect that the molecules are allowed to rapidly diffuse laterally across the membrane so that reactions can occur rapidly. This idea is very far from the real motion that characterizes cell membranes. On the contrary, the motion of membrane proteins is highly restricted and deviations from normal free diffusion are commonplace across different time and length scales. Physiological reasons for this behavior may be linked to the necessity of

biomolecular processes to be tightly regulated. Further, cell membranes are known to be densely crowded structures where the motion of macromolecules is inherently restricted. Unraveling the diffusion pattern of lipids and membrane proteins is critical to understanding the organization of many fundamental physiological processes. These processes include receptor recognition, transport to and from the cell membrane, and cell-to-cell communication. In general, diffusive transport on the cell membrane has key functions in signal transduction and in the way cells interact with their surroundings.

This review deals with the mechanisms underlying anomalies in the diffusion of membrane molecules. The remaining of Section 1 reviews general aspects of normal and anomalous diffusion. Section 2 overviews the different physical models that explain anomalous diffusion, with particular emphasis on how different models arise in the plasma membrane. Section 3 focuses on the experimental evidence that has accumulated over the last 30 years on membrane diffusion and its implications on the mechanisms underlying anomalous diffusion.

1.1 Brownian motion and anomalous diffusion

Brownian motion, also known as Wiener process, is probably the most typical stochastic process in the physical sciences and engineering. Rigorously speaking, it is defined in one dimension as a continuous motion with independent and identically distributed Gaussian random displacements (Kuo, 2006). This definition has direct consequences on its properties. In particular, the mean square displacement (MSD) is linear with time. Brownian motion can be easily expanded to two or three dimensions by considering two or three independent processes, respectively. In a more physical context, Brownian motion develops when a molecule is constantly hit by other particles (for example, water molecules) and allowed to diffuse unrestrictedly as a consequence of the momentum transferred by collisions (Einstein, 1905). As such, Brownian motion is the solution to the diffusion equation

$$\frac{\partial P}{\partial t} = D\left(\frac{\partial^2 P}{\partial x^2} + \frac{\partial^2 P}{\partial y^2}\right), \tag{1}$$

where D is the diffusion coefficient and P represents either the particle concentration or the probability of finding a particle at location (x, y) at time t. Equation (1) is written in two dimensions because we deal with diffusion in membranes, namely a two-dimensional environment.

Assuming the particle is at the origin at time zero, the solution to Eqn (1) is a Gaussian function

$$P(\mathbf{r}, t) = \frac{1}{4\pi Dt} e^{-r^2/(4Dt)}, \tag{2}$$

where $r^2 = x^2 + y^2$ and the space integral under $P(\mathbf{r}, t)$ at any given time is unity because we solve for a single particle. Thus $P(\mathbf{r}, t)$ is the probability of finding the particle at location $\mathbf{r}$ at time t after starting from the origin. $P(\mathbf{r}, t)$ is a propagator since it describes the temporal evolution and, given the fundamental solution (Eqn (2)), one can construct the general solution for any initial conditions. From Eqn (2), we see that the MSD is

$$\langle r^2 \rangle = \int_0^\infty (2\pi r) P(\mathbf{r}, t) r^2 dr = 4Dt. \tag{3}$$

Note that in one and three dimensions the solutions for the MSD are $2Dt$ and $6Dt$, respectively. Thus the hallmark of "normal" diffusion is a square displacement that on average increases linearly in time.

A system is typically considered to exhibit anomalous diffusion when Eqn (3) breaks down. In general, it is possible that the MSD increases faster or slower than the linear solution. The most common situation is

$$\langle r^2 \rangle = Kt^\alpha, \tag{4}$$

where α is the anomalous exponent, and K is a generalized diffusion coefficient with units of $\mathrm{cm}^2/\mathrm{s}^\alpha$. The process is subdiffusive when $\alpha < 1$ and superdiffusive when $\alpha > 1$. When $\alpha = 1$, "normal" diffusion is recovered. Other functional forms have been theoretically derived, e.g., an exponential time dependence (Cherstvy & Metzler, 2014), but this chapter deals primarily with subdiffusive processes of the form $MSD{=}Kt^\alpha$ where $\alpha < 1$.

2. MODELS FOR ANOMALOUS DIFFUSION

Anomalous diffusion can be described with different models (Bouchaud & Georges, 1990; Ralf Metzler, Jeon, Cherstvy, & Barkai, 2014). Among these, we find fractional Brownian motion (fBM), continuous time random walks (CTRWs), and obstructed diffusion, which have been extensively used to model diffusion in living cells (Höfling & Franosch, 2013). One of the most challenging aspects of anomalous diffusion is that different processes yield the same MSD (Eqn (4)). Here we provide a survey

for the most common subdiffusion models, by describing their fundamental properties and we attempt to explain how these models may arise in the plasma membrane environment of a living cell.

2.1 Fractional Brownian motion

fBM is the archetypal subdiffusion process due to the simplicity and probably the elegance of its mathematical definition. fBM is defined via a generalization of Brownian motion, where the increments are no longer independent but they depend on previous increments (Mandelbrot & Van Ness, 1968). In one dimension, the position obeys the autocorrelation function

$$\langle x(t)x(t+s)\rangle = \frac{K}{2}[t^{\alpha} + (t+s)^{\alpha} - s^{\alpha}], \tag{5}$$

where t and s are positive times and α is the anomalous exponent as described before (Figure 1). Again, $\alpha = 1$ yields independent increments, i.e., Brownian motion. Often fBM is expressed in terms of the Hurst exponent H, with $2H = \alpha$. As in standard Brownian motion, the propagator of this process is also Gaussian, but with a time-dependent diffusion coefficient (Sebastian, 1995). In other words, Eqn (2) is modified so that $\langle x^2\rangle = Kt^{\alpha}$,

$$P(x,t) = \frac{1}{\sqrt{2\pi Kt^{\alpha}}} e^{-x^2/(2Kt^{\alpha})}. \tag{6}$$

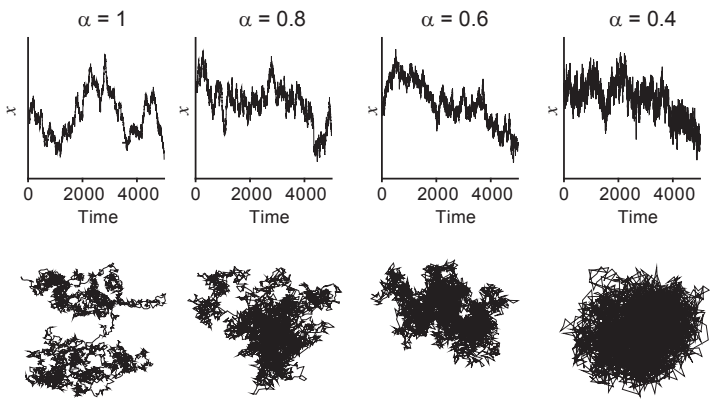

Figure 1 Numerical simulations of fractional Brownian motion in two dimensions for different α exponents between 0.4 and 1. $\alpha = 1$ is normal Brownian motion. Each trajectory is simulated for 5000 steps. The top panels are fractional Brownian motion in one dimension which is the *x* displacement of the trajectories seen in the bottom panels.

The extension of fBM to two dimensions is not as straightforward as the case of Brownian motion. To the best of our knowledge, there is currently no consensus as to what is the best way to define a 2D fBM, and typically it is described in terms of two independent fBM along the two dimensions.

In spite of the relative simplicity of the mathematical definition of fBM, describing it in terms of a physical mechanism is not trivial. A feasible origin for fBM is diffusion in a viscoelastic medium, which can arise from very densely crowded environments (Bronstein et al., 2009; Ernst, Hellmann, Kohler, & Weiss, 2012; Goychuk, Kharchenko, & Metzler, 2014; Szymanski & Weiss, 2009). In an elastic material such as a perfect spring, the stress is proportional to strain, i.e., the restoring force linearly increases with the deformation length. On the other hand, in a viscous material such as honey, the force exerted on an object, opposing its motion, is proportional to its velocity and independent of the distance it moves, with the proportionality constant termed the viscous drag coefficient ζ. The fluctuation-dissipation theorem tells us the diffusion coefficient in a viscous material is inversely proportional to the viscous drag coefficient, $D = k_B T/\zeta$. A viscoelastic material has both elastic and viscous properties; thus the restoring force depends on velocity and displacement. As a consequence, the material applies a restoring force against deformation that has memory in the sense that it depends on how much time passed since the initial deformation was applied. Eventually, the material relaxes into a new conformation and the restoring force decays to zero. In a viscous medium, a particle experiences a friction force in the opposite direction to its velocity independent of its past and thus it undergoes Brownian motion. However, a particle in viscoelastic medium experiences forces in both the direction opposite to the instantaneous velocity and in the direction to where it came from because the particle motion locally deforms the medium. As a consequence, the motion is antipersistent and it has a tendency to go back to the locations it visited in the past. This type of antipersistent motion can be modeled as fBM where the smaller the exponent α, the more compact is the motion. In other words, the higher α, the sparser the explored space (see Figure 1). An equivalent picture of elastic and viscous materials is that of solids and liquids, whereas a solid stores mechanical energy while a liquid dissipates it. A viscoelastic material both stores and dissipates energy.

Complex systems can exhibit rich viscoelastic behavior (Mason & Weitz, 1995). What specific phenomena may confer viscoelastic properties to the plasma membrane? At least three physical effects can induce viscoelasticity: (1) *Macromolecular crowding*. This is the best established mechanism for viscoelasticity in relation to anomalous diffusion (Guigas, Kalla, & Weiss, 2007;

Weiss, 2013). Let us envision the plasma membrane as a solvent densely packed with molecules of different sizes. As a tracer particle moves by diffusion in this medium, other molecules leave space for its path as dictated by thermal fluctuations. However, the sea of other molecules presses to close this space introducing an elastic effect. As time evolves, macromolecules relax in the new location and the elastic effect disappears. (2) *Transient interactions with cytoskeletal components*. In this scenario, interactions of different strengths maintain specific positions of the plasma membrane highly localized in space (Chichili & Rodgers, 2009; Luna & Hitt, 1992). Deformation of the plasma membrane introduces forces at these locations. Provided that these interactions are reversible, the membrane relaxes over time as the interactions break. (3) *Intermolecular interactions*. Interactions among membrane components can lead to short-range order in a fluid (Marguet, Lenne, Rigneault, & He, 2006). Thus, as the membrane is deformed, a short-range elastic effect gives rise to memory in the motion of tracer particles.

2.2 Continuous time random walk

A random walk consists of random steps forming a path, where, for example, each step occurs at equally spaced times. Thus, the waiting time between jumps is a constant. When the step size either involves a constant distance or is a random variable with finite mean and variance, the random walk converges in the long time limit to Brownian motion. In particular, we have that for a 1D random walk of mean step size L, $\langle x^2 \rangle = L^2 N$ after N steps, which is equivalent to Eqn (3).

Random walks can also be considered when steps take place at random times. We can then define a CTRW as a random walk with sojourn times between steps being random variables according to a distribution $\psi(\tau)$ for times $\tau > 0$. Again, when $\psi(\tau)$ has finite mean and variance, e.g., an exponential distribution with characteristic time τ_0, the average number of steps in time t is t/τ_0 and we recover normal diffusion at times $t \gg \tau_0$ with $\langle x^2 \rangle = (L^2/\tau_0)\, t$. Thus, we have a diffusion process, with a coefficient $D = L^2/2\tau_0$.

The situation changes dramatically when the distribution of waiting times between steps is scale free, such as a power-law distribution (Scher & Montroll, 1975; Scher, Shlesinger, & Bendler, 1991)

$$\psi(\tau) \sim \tau^{-(1+\alpha)}. \tag{7}$$

As we will see later, this type of power-law distributions has been measured in the immobilization times of membrane proteins (Weigel, Simon,

Tamkun, & Krapf, 2011). When $0 < \alpha < 1$, the mean of the waiting time diverges and thus we cannot define a characteristic time τ_0 as before. Instead, the only characteristic time of the process is the total time over which the experiment is conducted. As a consequence, experimental results depend on measurement time, a problem that will be discussed later.

Before describing the properties of random walks with power-law waiting times, let us discuss the reasons for such distributions to exist in the membrane of a living cell. First, we note that a CTRW is an excellent model for the motion of a particle that alternates between mobile and immobile periods. Here, the process may be described by random steps (mobile segments of the trajectory) that take place at random times (with waiting times defined as the time spent in the immobile phase). Immobilization can occur through binding to a cytoskeletal component or to a macromolecular complex, yielding long periods between steps. However, binding kinetics typically have a specific dissociation coefficient k, which yields a dissociation time with an exponential distribution

$$\psi(\tau) = k \exp(-k\tau). \tag{8}$$

Therefore, for times $t \gg 1/k$, this process exhibits normal diffusion.

Two situations can give rise to heavy-tailed (power law) CTRWs: nonstationary interactions and heterogeneous interactions.

2.2.1 Time evolution route to heavy-tailed CTRW

In the first scenario, a protein transiently binds to a macromolecular complex that grows over time and as a consequence, the dissociation coefficient changes. If we assume the escape probability decreases with time, we can postulate a model where the dissociation coefficient is $k(t) = \alpha/(t + t_0)$ and t_0 is a nucleation time for the macromolecular complex (Weigel, Tamkun, & Krapf, 2013). The survival probability P_s, i.e., the probability that the protein has not escaped after a time t obeys the rate equation:

$$\frac{dP_s}{dt} = -\frac{\alpha}{(t+t_0)} P_s, \tag{9}$$

which has a power-law solution $P_s(t) = t_0^{\alpha}(t+t_0)^{-\alpha}$. We can now obtain the residence time probability density function, i.e., the distribution of dissociation times,

$$\psi(\tau) = -\frac{dP_s(\tau)}{d\tau} \sim \tau^{-(1+\alpha)} \tag{10}$$

with the form of Eqn (7).

2.2.2 Heterogeneous interactions route to heavy-tailed CTRW

The second situation for which a heavy-tailed CTRW can arise consists of interactions with different complexes that translate into a distribution of dissociation coefficients (Burov, Jeon, Metzler, & Barkai, 2011; Klafter & Sokolov, 2005). In this case, we start from a narrow distribution of binding energies E_B such that

$$P(E_B) = \alpha \exp(-\alpha E_B),$$

where E_B is expressed in units of k_BT. Following Arrhenius rate law, the dissociation coefficient from an individual complex with binding energy E_B is $k = k_0 \exp(-E_B)$ and, therefore, the distribution of dissociation coefficients is $P(k) = \alpha\, k_0^{-\alpha} k^{\alpha-1}$ with $0 < k < k_0$. For a given dissociation coefficient k, the conditional waiting time probability is $P(\tau|k) = k \exp(-k\tau)$. By integration, we obtain the power law *a priori* distribution $P(\tau) = \int_0^{k_0} k \exp(-k\tau) P(k) dk$,

$$P(\tau) = \frac{\alpha}{k_0^{\alpha}} \gamma(\alpha+1, k_0\tau)\tau^{-(1+\alpha)}, \tag{11}$$

where $\gamma(s,t)$ is the lower incomplete gamma function $\gamma(\alpha+1, t) = \int_0^t \tau^{\alpha} e^{-\tau} d\tau$. For long times, $\gamma(\alpha+1, k_0\tau) \to \Gamma(\alpha+1)$ and $P(\tau)$ converges to the heavy-tailed power law $P(\tau) \sim \tau^{-(1+\alpha)}$.

Heavy-tailed CTRW have anomalous diffusion properties that greatly differ from those of fBM. Let us consider a measurement of a particle over a time t_1 that diffuses within the framework of a heavy-tailed CTRW. Given that all waiting times are possible, within this measurement time, we will likely observe the particle having at least one long waiting time of the same order of magnitude of the time t_1. However, if we measure over much longer times, the particle will probably display a waiting time within the observation time t_2 much longer than that observed within t_1. Three consequences stem from this concept.

2.2.3 Nonstationarity

The longer the observation time, the longer the effective average time the particle is immobilized and the process is not stationary (Metzler & Klafter, 2000). In other words, as measurement time progresses, the rate of jumps decreases and thus the apparent diffusion coefficient goes down, i.e., the system ages with time. This phenomenon is due to the fact that the expected value of the immobilization time diverges, $\langle\tau\rangle = \int_0^{\infty} \tau\psi(\tau) d\tau = \infty$. However, any physical measurement takes place in a finite time t_m and the

observed effective immobilization time is $\langle\tau\rangle_{eff} = \int_0^{t_m} \tau\psi(\tau)d\tau$, which is bounded by t_m. This puzzling observation means that the measurement time affects the estimated diffusion coefficient.

2.2.4 Irreproducibility of results

Because one long waiting time of the order of the experimental time is typically observed, the measured parameters depend on a single random variable and the temporal averages remain random, even in the long time limit. As a consequence, different particles display a very broad distribution of estimated diffusion coefficients, no matter how long the observation time is. In terms of probability theory, because the variance diverges, the classical central limit theorem breaks down (Peebles, 1987).

2.2.5 Weak ergodicity breaking

In traditional systems, we estimate parameters by averaging measurements. For example, from measurements of MSD we can estimate the diffusion coefficient. Such estimates can be obtained by averaging over many different particles or alternatively by measuring a single trajectory that explores the whole phase space. Often, in single-particle tracking experiments, it is difficult to obtain a very large number of trajectories so that averages can be performed over an ensemble. Instead, averages are obtained for individual trajectories by averaging over time. For a random walk that visits the locations $\mathbf{r}_i$ with $i = 1,2,\ldots,N$ (here N−1 represents the number of steps), we define the time-averaged MSD for a lag time u as

$$\overline{\delta^2}(u) = \frac{1}{N-u}\sum_{i=1}^{N-u}(\mathbf{r}_{i+u} - \mathbf{r}_i)^2, \tag{12}$$

where δ^2 is the square displacement and the bar represents a temporal average. Note that u is the lag time expressed in number of steps, which is converted to real time units in a straightforward way $\Delta = ut_0$, where t_0 is the step time. The convergence of the temporal averages at long times to the ensemble average is known as the ergodic hypothesis. In a CTRW, the ergodic hypothesis breaks down and the time average does not converge to the ensemble average, independent of the measurement time. Further, for the power-law waiting time distribution, the time and ensemble mean-squared displacements have different dependence on lag time (He, Burov, Metzler, & Barkai, 2008; Lubelski, Sokolov, & Klafter, 2008). In this case, we obtain

$$\overline{\delta^2} \sim \Delta \tag{13}$$

but

$$\left\langle x^2 \right\rangle \sim t^{\alpha}. \tag{14}$$

We employ brackets as ensemble average and the bar as temporal average. Therefore, when the MSD is computed for an individual trajectory, the diffusion process appears "normal" in the sense that it scales linearly with lag time. Nevertheless, the diffusion is anomalous and the ensemble average of the temporal MSD explicitly depends on experimental time (aging behavior) due to its nonstationary properties (He et al., 2008)

$$\left\langle \overline{\delta^2} \right\rangle \sim \frac{\Delta}{T^{1-\alpha}}, \tag{15}$$

where T is the experimental time. Here, the temporal MSDs are averaged over many trajectories because the individual MSDs remain random variables even in the long time limit.

2.3 Obstructed diffusion

One of the simplest scenarios for anomalous diffusion we can conceptually envision is when the motion takes place in an environment that is densely packed with immobile objects. As the concentration of immobile obstacles increases, the available space decreases and diffusion becomes more and more restricted. At high concentrations, the obstacles form clusters that block the free motion of particles. Scaling relations have been derived for the average cluster size as a function of obstacle concentration (Ben-Avraham & Havlin, 2000) showing that the cluster size increases as a power law. At a critical concentration, a percolation transition takes place and a cluster that traverses the whole space forms. Thus the underlying medium is partitioned into disconnected regions. As the obstacle concentration approaches the percolation transition, a diffusing particle can explore the whole space, but its diffusion is constantly hindered. In this situation, the obstacles form an intricate maze where dead ends and cul-de-sacs appear over many length scales. Thus a particle diffusing in a percolating structure often has to retrace itself giving rise to anomalous diffusion with a compact exploration pattern (Figure 2(A–C)).

When the obstacle concentration is much smaller than criticality, the cluster sizes are small and transient anomalous diffusion is observed only over small length scales. Thus the MSD is sublinear over short times and linear at longer times (Figure 2(A)) (Saxton, 1996; Weigel, Ragi, et al., 2011). The subdiffusive regime grows as concentration increases and

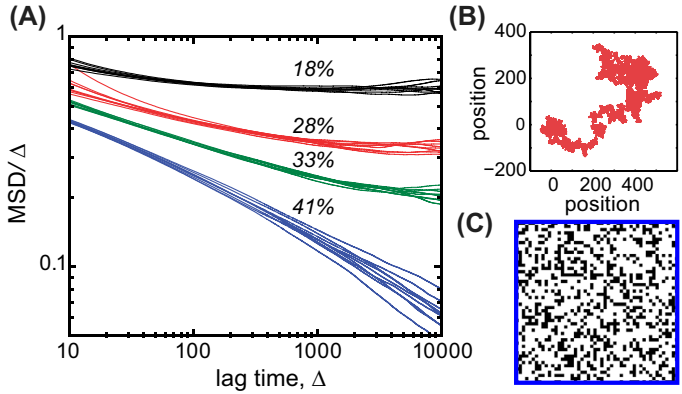

Figure 2 Simulations of obstructed diffusion. (A) Temporal MSD/Δ, i.e., $\overline{\delta^2}/\Delta$, as a function of Δ in a log–log plot for individual simulated tracers in the presence of immobile obstacles at different concentrations, where Δ is the lag time. Several simulations are presented for each obstacle concentration in order to show the small scatter of the mean square displacement (MSD). Simulations are performed in square lattices using a Monte Carlo blind ant algorithm (simulation details can be found in Weigel, Ragi, et al., 2011) so that 41% obstacles is right above the percolation threshold. The simulations with 41% obstacles show anomalous diffusion over the whole simulated time, but all other concentrations exhibit transient subdiffusion with a time upon which the process exhibits normal diffusion, i.e., MSD/Δ becomes flat, as expected from MSD ∼ Δ. (B) Example of a trajectory of 10^6 steps in a square lattice with 33% of sites obstructed. (C) Example of a 50 × 50 region of a square lattice where 33% of the sites are obstructed (dark pixels). Note that the region shown is only a small fraction of the lattice used to obtain trajectories with 10^6 steps.

when criticality is reached subdiffusion is observed at all length scales. At criticality, the obstacle mesh forms a random fractal with a noninteger dimension smaller than the dimension of the embedding space, i.e., $d_f < 2$. As mentioned above, the MSD is linear for any integer dimension (Eqn (3)), but this rule does not hold when diffusion takes place in a medium with fractal dimension (Ben-Avraham & Havlin, 2000).

Many similarities are shared between fBM and obstructed diffusion. Among them, the temporal averages converge to the ensemble average, the increments are stationary, and the exploration is more compact than in Brownian motion. None of these effects hold for the heavy-tailed CTRW. Nevertheless, the distinction between these stationary processes and a CTRW is not trivial because convergences can be extremely slow, a challenge that requires special attention (Burnecki et al., 2012; Deng & Barkai, 2009; Kepten, Bronshtein, & Garini, 2011; Magdziarz, Weron, Burnecki, & Klafter, 2009). Similarly, while subdiffusion in a percolation

cluster at a concentration below criticality is transient, the convergence to normal diffusion can be slow, i.e., subdiffusion may be observed over several orders of magnitude. One clear distinction between fBM and obstructed diffusion is that while the propagator of fBM is Gaussian (Eqn (6)), the propagator for diffusion in a percolation cluster is not (see Eqn (4) in Weigel, Ragi, et al. (2011)).

2.4 Heterogeneous Landscapes

It has long been appreciated that beyond energy disorder, spatial heterogeneities can lead to complex dynamics (Havlin & Ben-Avraham, 1987). However, the extent of the complexity of motion in a heterogeneous environment has only been recently recognized. It was demonstrated that a heterogeneous diffusion process (HDP) with space-dependent diffusion coefficient can exhibit weak ergodicity breaking (EB) (Cherstvy, Chechkin, & Metzler, 2013). Cherstvy et al. (2013) showed that a Markovian HDP with power-law space dependence of the diffusion coefficient, $D(x) \sim D_0|x|^{\gamma}$, yields anomalous diffusion where the ensemble-averaged MSD scales as $\langle \delta^2 \rangle \sim t^{2/(2-\gamma)}$ but the time-averaged MSD remains linear in the lag time, $\overline{\delta^2} \sim \Delta$. Thus, the process is nonergodic in a similar fashion to a CTRW (see Eqns (13) and (14)), even though the mechanism is vastly different. This HDP leads to subdiffusion when $\gamma < 0$ and superdiffusion when $\gamma > 0$, but both cases give rise to nonergodic behavior with a large scatter in the time-averaged MSD. Cherstvy and Metzler (2014) studied in detail the amplitude scatter between individual realizations and the special case of the critical point when $\gamma = 2$. At this critical point, the fluctuations in the temporal MSD diverge and the ensemble-averaged MSD no longer follows a power law. Instead, for $\gamma = 2$, the MSD exhibits an exponential growth $\langle \delta^2 \rangle \sim \exp(2D_0 t)$.

A new model for HDP where the diffusivity varies randomly but it is constant within patches of random sizes was introduced by Massignan et al. (2014). This model was developed due to the resemblance of random patches to the rapidly varying diffusivity observed on the cell surface (Cutler et al., 2013; Giannone et al., 2010; Masson et al., 2014; Serge, Bertaux, Rigneault, & Marguet, 2008). Similar to the HDP with power-law space dependence of the diffusion coefficient (Cherstvy & Metzler, 2014), ergodicity breaking is found. The key component of this model is a heavy-tailed distribution of the residence time in different patches that can be achieved by a power-law distribution of patch sizes. The HDP model with random

patches was found to be particularly relevant to the diffusion of DC-SIGN in the plasma membrane as discussed later (Manzo et al., 2015).

2.5 Subordination Schemes

So far, the discussed models for anomalous diffusion describe specific mechanisms. However, given that the plasma membrane is a highly complex environment (see Figure 3), different mechanisms can coexist. Therefore, different models should be combined into a stochastic process of increased complexity. Such a problem can be considered within a subordination scheme (Blumen, Klafter, White, & Zumofen, 1984; Fogedby, 1994; Klafter, Blumen, & Zumofen, 1984; Meroz, Sokolov, & Klafter, 2010; Sokolov & Klafter, 2005). For example, we can treat an fBM in the operational time as discussed before and then place it in a laboratory time where each step is drawn from a power-law distribution (Klafter & Sokolov, 2011; Tabei et al., 2013). Thus, we have fBM subordinated to a CTRW.

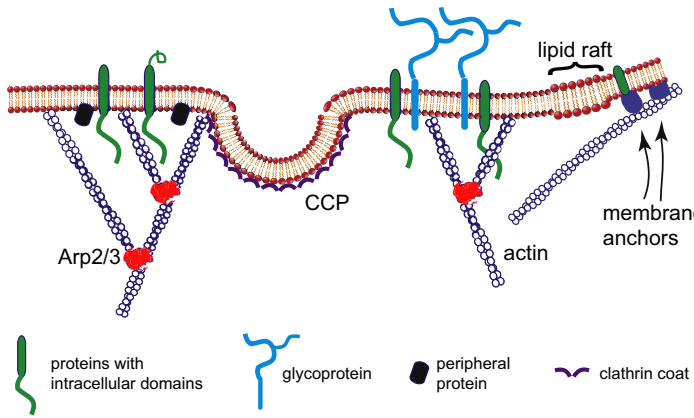

Figure 3 Largely simplified sketch of the plasma membrane. In this illustration, actin filaments can link to the plasma membrane and obstruct the motion of proteins. Two types of membrane anchors are shown, proteins that bind actin directly to the membrane (e.g., annexins) and to proteins, such as talin and vinculin, that connect actin to cell adhesion receptors, such as integrins (Winder & Ayscough, 2005). Membrane proteins may also have intracellular domains that contribute to interactions with cytoplasmic filaments such as the cortical actin. Extracellular carbohydrate chains (e.g., glycoproteins) can also contribute to interactions among themselves or with the extracellular matrix. A clathrin-coated pit (CCP) is shown where molecules with specific recognition sites can be captured. In addition, the high density of different membrane proteins contributes to its complexity. Transient functional domains such as cholesterol-rich lipid rafts also partition the membrane into regions with different diffusive behavior. (See color plate)

The statistics of subordinated processes are not trivial and each case requires special attention. Meroz et al. (2010) have considered the coexistence of diffusion on a fractal and a heavy-tailed CTRW. This is a special case of subordinating an ergodic anomalous process to a nonergodic one and it is particularly relevant to diffusion on the cell membrane as discussed later (Weigel, Simon, et al., 2011). The fractal structure models spatial obstruction to the motion of membrane proteins and the CTRW can represent immobilization due to trapping into macromolecular complexes. This process is found to exhibit aging and weak ergodicity breaking. The MSD is found to scale as

$$\left\langle x^2 \right\rangle \sim t^{\alpha\beta} \tag{16}$$

and

$$\left\langle \overline{\delta^2} \right\rangle \sim \frac{\Delta^{1-\alpha+\alpha\beta}}{T^{1-\alpha}}, \tag{17}$$

where the two constants α and β characterize the heavy-tailed CTRW and the fractal random walk subdiffusive exponents, respectively. As before, we denote with a bar $\overline{\delta^2}$ a moving temporal average over a single trajectory of time T and with brackets $\langle x^2 \rangle$ the ensemble average. Aging behavior is evident in the dependence of the MSD on the experimental time. Furthermore, the temporal MSD of individual trajectories $\overline{\delta^2}$ is found to exhibit a large scattering due to the nonergodic properties of the CTRW (Meroz et al., 2010).

A subordination scheme is an elegant way to solve for the simultaneous effect of two different subdiffusion models. However, this scheme has some limitations. For example, an fBM has memory, which is now considered in space but the temporal relaxation due to a particle remaining for a long time at a specific location is neglected.

3. EVIDENCE FOR ANOMALOUS DIFFUSION IN THE PLASMA MEMBRANE

The analysis of diffusion in living cells has to be placed in a specific length- and time-scale range. Diffusion in an amorphous material can be measured without tangible theoretical limitations beyond the time for a material to crystallize which is usually not within experimental reach. However, diffusion in living cells can only be reasonably measured for times smaller than its lifetime or the time until cell replication occurs. Thus,

whenever we discuss power-law distributions, they are meant to occur within reasonable times. Obviously, these distributions will change for times upon which the system is altered. Further, the situation in a typical living cell is much more complex than in amorphous materials because it can involve several phases. As a result, different stochastic mechanisms govern diffusion in cellular environments at different timescales. For example, the motion of lipid granules in fission yeast was shown to be best described by CTRW subdiffusion with features of ergodicity breaking at short times (in the ms range) and by a mechanism closest to fBM at longer times (Jeon et al., 2011).

Anomalous diffusion in the membrane of living cells has been observed in a very broad variety of cell types. Both membrane proteins and lipids undergo anomalous diffusion in different cells including human embryonic kidney, neurons, Chinese hamster ovary, Cos7, fibroblasts, keratinocyte, mouse hepatoma (HEPA-OVA), sperm, and HeLa (James, Hennessy, Berge, & Jones, 2004; Kusumi et al., 2005; Manley et al., 2008; Murase et al., 2004; Ritchie, Iino, Fujiwara, Murase, & Kusumi, 2003). Further, anomalous diffusion of membrane proteins was also observed in living animals such as zebrafish (Schaaf et al., 2009). The purpose of this chapter is not the extensive discussion of the phenomena observed in different cell types and for different membrane molecules, but to discuss at a higher level the mechanisms responsible for the observed anomalous diffusion. For details on experimental work on different proteins and cell lines, the reader is referred to a recent review by Gal, Lechtman-Goldstein, and Weihs (2013).

As discussed above, some of the main physical mechanisms leading to subdiffusive motion involve intermolecular interactions within the membrane or with cytoskeletal components. These components include actin (Andrews et al., 2008; Heinemann, Vogel, & Schwille, 2013), cytoskeleton anchoring proteins (Bennett & Gilligan, 1993; Meier, Vannier, Serge, Triller, & Choquet, 2001; Winder & Ayscough, 2005), the extracellular matrix (Jiang, English, Hazan, Wu, & Ovryn, 2015; Torreno-Pina et al., 2014), clathrin-coated pits (CCP) (Weigel et al., 2013), lipid rafts (Eggeling et al., 2009), and the endoplasmic reticulum (Anderluh et al., 2014; Cui-Wang et al., 2012; Wu, Covington, & Lewis, 2014) (see Figure 3 for some examples).

3.1 Molecular dynamics simulations—nanoseconds to microseconds

The shortest timescales for diffusion in membranes have been studied by large-scale molecular dynamics simulations. These simulations investigate the behavior of lipids and proteins in small membrane patches with different

lipid compositions (Javanainen et al., 2013). The membranes of live cells are extremely crowded with proteins. For example, the area occupied by proteins in the membrane of red blood cells was measured to be at least 23% (Dupuy & Engelman, 2008). It is generally estimated that the area fraction of proteins in the cell membrane can reach up to 50% (Casuso et al., 2012). Thus, simulations are also performed with different protein concentrations to identify and isolate protein crowding effects. Further, the packing of lipids in the plasma membrane is sensitive to lipid chemistry and cholesterol concentration. In particular, introducing cholesterol and sphingolipids into a lipid bilayer forms a liquid ordered phase with a higher packing density, thus the diffusivity in membranes with higher cholesterol concentrations decreases (Almeida, Vaz, & Thompson, 1992).

Jeon, Monne, Javanainen, and Metzler (2012) performed a detailed stochastic analysis of molecular dynamics simulations in lipid bilayers. Their work focused on the effect of cholesterol on subdiffusion and understanding whether the motion of lipids can be better modeled by a CTRW or by anticorrelated motion such as fBM or fractional Langevin equations. Strikingly, it was found that in the presence of cholesterol, lipids exhibit subdiffusive behavior up to times of the order of hundreds of nanoseconds before a transition to normal diffusion is observed. This timescale is much longer than what was previously estimated. In particular, these results are surprising because model membranes lack the complexity of the interactions with the cytoskeleton or with large protein assemblies. Thus, in native cell membranes, the subdiffusion regime probably stretches even further, into macroscopic timescales. The stochastic analysis described in Jeon et al. (2012) includes the scattering of the mean squared displacement, stationarity, the displacement autocorrelation function, and moment ratios. These tools show that the motions of lipids and cholesterol are ergodic processes, universally consistent with a fractional Langevin equation. Often, the ergodicity breaking parameter, which quantifies the fluctuations of the MSD, is used to characterize ergodicity breaking (He et al., 2008),

$$EB = \frac{\left\langle \left(\overline{\delta^2} \right)^2 \right\rangle - \overline{\langle \delta^2 \rangle}^2}{\overline{\langle \delta^2 \rangle}^2}. \tag{18}$$

Note that the ergodicity breaking parameter is the variance of the normalized dimensionless MSD, $\chi = \overline{\delta^2}/\overline{\langle \delta^2 \rangle}$, thus it quantifies the fluctuations of the trajectories. If $EB = 0$ in the long time limit, we have ergodic behavior. It

was found the ergodicity breaking parameter decays to zero as time increases and thus the process is ergodic (Jeon et al., 2012). Akimoto, Yamamoto, Yasuoka, Hirano, and Yasui (2011) analyzed a closely related metric for the relative fluctuations of the MSD in the trajectory of lipids from molecular dynamics simulations. The relative fluctuations are defined as

$$R = \frac{\left\langle \left| \overline{\delta^2} - \overline{\langle \delta^2 \rangle} \right| \right\rangle}{\overline{\langle \delta^2 \rangle}}. \tag{19}$$

Similar to the ergodicity breaking parameter, the relative fluctuations R decayed to zero in the long time limit which indicates ergodicity. However, it was found that the decay was slower than expected from a Gaussian process. Akimoto et al. (2011) suggested the non-Gaussianity is caused by trapping times distributed according to power laws. Intriguingly, such a behavior would cause a dependence of the time-averaged MSD on experimental time, but no such dependence was found (Jeon et al., 2012).

The analysis of lipid and protein lateral diffusion at different crowding levels was analyzed by Javanainen et al. (2013) to unravel the roles of lipid packing and protein crowding. In that work, simulations were performed in two different systems: one preferring protein aggregation (dipalmitoylphosphatidylcholine, DPPC) and another one avoiding it (dilinoleoylphosphatidylcholine, DLPC). In both systems, when proteins are sparse, lipids exhibit anomalous diffusion for times up to 100 ns. Nevertheless, for intermediate protein crowding (1:200 to 1:100 proteins per lipid), subdiffusion is observed for times up to 10 μs in aggregating protein systems (DPPC) and up to 1 μs in nonaggregating systems (DLPC). For high protein crowding levels similar to those estimated to be relevant to live cells (1:75 to 1:50 proteins per lipid), subdiffusion is observed for strikingly long times. In fact, the subdiffusion timescales exceed those enabled by molecular dynamics simulations even employing coarse graining. From the data collected in Javanainen et al. (2013), it is estimated that normal diffusion would only be achieved at times of the order of several hundred microseconds or even milliseconds for protein aggregating systems and between 10 and 100 μs for nonaggregating systems.

3.2 Obstructed (hop) diffusion—microseconds to seconds

3.2.1 *Fluorescence recovery after photobleaching and optical tweezers*

The concept of membrane proteins being corralled by cytoplasmic fences (cortical actin or actin binding proteins sketched in Figure 3) is one of the

oldest and most studied mechanism for deviations from Brownian diffusion in the plasma membrane (Sheetz, 1983; Tsuji & Ohnishi, 1986). In this model, the part of the cytoskeleton in close proximity to the plasma membrane blocks the path of membrane proteins due to steric hindrance. One of the earliest experiments showing that cytoplasmic components introduce barriers to the lateral diffusion of membrane proteins involved measurements in cell blebs (Tank, Wu, & Webb, 1982). Blebs are spherical protrusions that form under specific conditions in eukaryotic cells. These structures resemble small balloons being inflated out of a plasma membrane patch and what makes them particularly useful for investigating the effect of the cytoskeleton on membrane diffusion is that they lack any actin cytoskeleton (Cunningham, 1995). Thus, differences between the diffusion properties of transmembrane proteins in blebs and those in membrane regions outside blebs can be attributed to the effect of the cytoskeleton in the vicinity of the plasma membrane, i.e., the cortical cytoskeleton. Using fluorescence recovery after photobleaching (FRAP), Tank et al. (1982) showed that in blebs, the lateral constraints to diffusion are released and, in turn, the diffusivity of receptors is enhanced.

Besides FRAP measurements, early evidence pointing to the existence of cytoplasmic barriers to the diffusion of membrane proteins came from optical tweezers measurements (Edidin, Kuo, & Sheetz, 1991; Edidin, Zuniga, & Sheetz, 1994; Kusumi & Sako, 1996). Proteins tagged with either gold or latex nanoparticles were dragged along the plasma membrane in a controlled manner using optical tweezers. The nanoparticle is captured in a three-dimensional optical trap and moved along the membrane until the protein bound to the nanoparticle encounters a barrier that causes it to escape from the trap. Thus, a measurement of the barrier free path (BFP) is obtained for each molecule. BFP and FRAP measurements indicate that the length upon which membrane proteins extend within the cytoplasm has dire consequences on the extent their path is obstructed (Edidin et al., 1994). These observations can be explained in terms of a cortical actin structure that lies close to the membrane but is not tightly bound. Thus, proteins with longer cytoplasmic domains encounter barriers more often and have increased difficulties in traversing such barriers.

Optical tweezers studies also shed light on the fluctuations and the mechanical properties of the cortical cytoskeleton (Sako & Kusumi, 1995). Thermal fluctuations introduce two different mechanisms by which membrane proteins can permeate through cytoplasmic barriers. On one hand, the actin cytoskeleton has a dynamic nature and it may exhibit fluctuations both in the lateral and in the normal directions. A barrier that retracts from the

membrane due to thermal fluctuations may leave enough space for the protein to cross through it, or in other words, the barrier is temporarily lifted. A second mechanism by which proteins can cross through a barrier is by fluctuations in the conformation of their cytoplasmic domains. Many membrane proteins are believed to have disordered cytoplasmic tails which would resemble a random coil. Thus spontaneous fluctuations cause the tail to shrink and allow the protein to cross the barrier.

3.2.2 Single-particle tracking

The ultimate method for studying the motion of proteins in the plasma membrane is through single-molecule tracking. Here the protein of interest is tagged with a marker that can be localized with nanometer precision. Useful markers include gold nanoparticles, fluorescent proteins, organic fluorophores, and quantum dots (QD). Tracking individual fluorescent proteins is often termed single-molecule tracking, while tracking gold nanoparticles or QDs is usually termed single-particle tracking. Here we will use these terms interchangeable. Metal nanoparticles provide the advantage of allowing detection in times as short as microseconds using video-enhanced microscopy (de Brabander et al., 1991; Sheetz, Turney, Qian, & Elson, 1989). However, they are typically large ($\sim$40 nm) and interactions with the extracellular matrix are a concern. Fluorescent proteins can be genetically encoded for measurements in a live cell and are small, often yielding negligible interactions with other components. However, experiments show that the choice of fluorescent protein and expression level is important to avoid oligomerization, low affinity interactions between proteins that normally do not interact, and trafficking artifacts (Aguet, Antonescu, Mettlen, Schmid, & Danuser, 2013; Costantini, Fossati, Francolini, & Snapp, 2012; Snapp et al., 2003). The main disadvantage of single fluorescent proteins is that they photobleach and thus, long measurements are difficult to obtain. QDs provide the great advantage of allowing very long measurements, but they exhibit blinking, random fluctuations between bright and dark states causing arbitrary long periods where a molecule cannot be tracked (Michalet et al., 2005; Pinaud, Clarke, Sittner, & Dahan, 2010).

Single-particle tracking shows that membrane proteins explore small regions during periods of time that are statistically significantly longer than what would be expected from Brownian motion, before moving to explore a new region. These results are consistent with a model where proteins are temporarily confined by cytoplasmic barriers. Thus a protein is observed to reside within a region or compartment during a relatively long stochastic

time before it hops to a new compartment, a process usually called hop diffusion (Figure 4(A) and (B)). As a consequence, proteins observed during periods of time much shorter than the time between collisions with the compartment perimeter are expected to display normal diffusion, i.e., MSD $\sim \Delta$ (Figure 4(C)). If a protein is confined within a compartment such that the escape probability is zero, as time increases the MSD can only increase to a finite value and thus it converges to a value that depends on corral size and geometry (Saxton & Jacobson, 1997). Specifically,

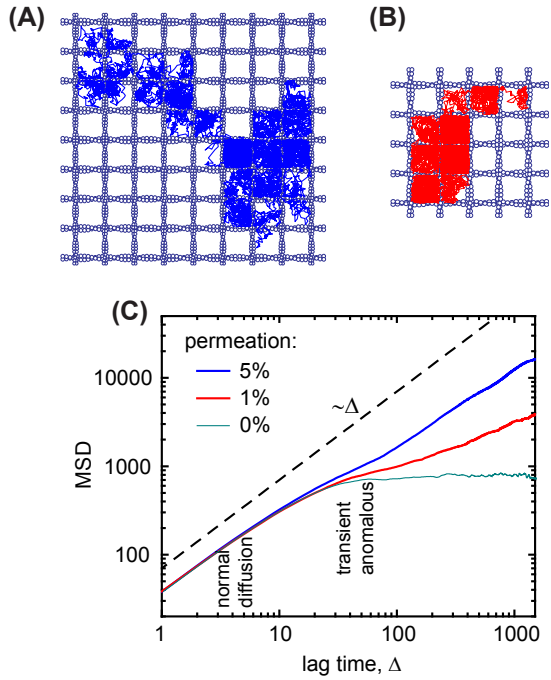

Figure 4 Fence model for transient anomalous diffusion. (A,B) Numerical simulations for random walks in the presence of permeable fences. The fences are sketched as actin filaments. These simulations are performed off-lattice with jumps drawn from a normal distribution with standard deviation $\sigma = 5$ in both x and y directions. The fences are placed a distance of 50 units from each other. Both trajectories are 10,000 jumps. The fences are permeable with a given probability of permeation: (A) 5% and (B) 1%. (C) Time-averaged mean square displacement (MSD) $\overline{(\delta^2)}$ for the trajectories shown in the upper panels as a function of lag time. At lag times much shorter than the hopping time, the MSD is linear. At intermediate times, a sublinear regime is observed and diffusion becomes normal again at longer times. The recovery of linear MSD is much slower for 1% permeation probability than for 5% permeation probability. A trajectory with no permeation through the fences (0% permeation probability), so that the trajectory is confined to a compartment, is also shown as a thin line. The dashed line indicates linear behavior (free diffusion), i.e., MSD $\sim \Delta$. (See color plate)

$\text{MSD} = \langle r_c^2 \rangle [1 - A_1 \exp(-4A_2 Dt/\langle r_c^2 \rangle)]$ where r_c is the compartment radius and A1 and A2 are constants related to the shape of the compartment, as seen in Figure 4(C). Note that, even though the MSD is not linear, this behavior is considered normal diffusion within a confined region. However, when the tracked molecule is allowed to escape by hopping to a different compartment, the MSD will again become linear at times longer than the escape time, albeit with a reduced diffusion coefficient. The new apparent diffusion coefficient is $D_a = r_c^2/\tau_0$ with τ_0 being the characteristic escape time. Thus, diffusion is transiently anomalous for intermediate times between the characteristic confinement time and the escape time. In this model, we assume the confining compartments cover the whole membrane, so that the compartment size is also the distance between the centers of the compartments. A different model can also be proposed where the compartments are patches within the membrane, so that the molecule diffuses freely between periods of confined diffusion. This latter model shares some of the properties of CTRW arising from energetic disorder and will be discussed in Section 3.5. A detailed review of the current understanding of the organization of the plasma membrane is provided in Akihiro Kusumi et al. (2012).

Transient subdiffusion with an MSD of the form seen in Figure 4(C), i.e., with linear/sublinear/linear regimes, corresponds to a narrow distribution of compartment sizes. Such a distribution is expected to yield a distribution of escape times close to an exponential distribution

$$\psi(\tau) = \tau_0^{-1} \exp(-\tau/\tau_0). \tag{20}$$

However, many experiments fail to produce an MSD with the linear, sublinear, and again linear regimes. Instead, membrane protein subdiffusion is often observed over extended periods of time (Feder, Brust-Mascher, Slattery, Baird, & Webb, 1996; Notelaers et al., 2014, 2012; Smith, Morrison, Wilson, Fernandez, & Cherry, 1999). The hop diffusion model is consistent with these observations if the compartment size distribution is assumed to be broad. The escape time, of course, depends on compartment size and thus it would also have a very broad distribution. In a simplified picture, the escape time for a given compartment radius r_c is an exponential as Eqn (20) with $\tau_0 = r_c^2/D_a$ where D_a is the apparent diffusion coefficient. Thus,

$$\psi(\tau) = \int_0^\infty \frac{D_a}{r_c^2} \exp\left(-D_a \tau / r_c^2\right) P(r_c) dr_c \tag{21}$$

where $P(r_c)$ is the distribution of compartment radii.

A special and interesting case arises when the cytoskeletal barriers produce a self-similar meshwork. In this case, we expect a scale-free distribution of compartment sizes and in turn a distribution of escapes without a characteristic time. Some experiments agree with predictions of this type of anomalous diffusion where a linear MSD regime is not attained (Smith et al., 1999; Weigel, Ragi, et al., 2011; Weigel, Simon, et al., 2011). A different view of diffusion within a scale-free meshwork is that of nested compartmentalization. As a molecule escapes from a small compartment it remains confined within a larger one. Therefore, confinement can occur within many length scales. Evidence for such motion was observed in the plasma membrane of rat kidney fibroblasts (Fujiwara, Ritchie, Murakoshi, Jacobson, & Kusumi, 2002; Suzuki, Ritchie, Kajikawa, Fujiwara, & Kusumi, 2005). The neutral lipid dioleoylphosphatidylethanolamine (DOPE) and transferrin receptors (TfR) were observed to hop between small compartments of the order of 250 nm and remain confined for longer times inside 750 nm compartments, displaying an effective nested double compartment structure (Fujiwara et al., 2002). Fujiwara et al. (2002) reported residence times of the order of 11 ms for the small compartments and 0.6 s for the larger compartments for DOPE, and 55 ms and 1.8 s for TfR. Similarly, Suzuki et al. (2005) observed a nested compartmentalization of G protein-coupled receptors (GPCRs) in rat kidney fibroblasts with compartment sizes of 210 and 730 nm. As compartments become smaller, the observation of confinement becomes challenging. A scale-free compartmentalization of a membrane can also be obtained with a high concentration of immobile obstacles that generate a percolation cluster (Ben-Avraham & Havlin, 2000; Deverall et al., 2005; Saxton, 1994). Membrane proteins and lipids tethered to the cytoskeleton behave as immobile obstacles, hindering diffusion (Murase et al., 2004; Nakada et al., 2003). The effects of immobile obstacles on the motion of membrane proteins are described above in Section 2.3.

Direct observations of actin forming physical barriers to the motion of receptors over timescales of seconds were obtained from simultaneous single-particle tracking of QD-labeled IgE receptors and imaging cortical GFP-tagged actin in live RBL cells. Andrews et al. (2008) observed large actin bundles in the proximity of the plasma membrane and simultaneously tracked QD-labeled receptors using both TIRF and confocal microscopy. TIRF measurements were performed at 33 frames/s and confocal measurements at 1 frame/s. Both measurements show that actin bundles create micrometer-sized dynamic compartments and that receptor motion remains

limited to actin-poor regions. The actin structure is observed to reorganize over timescales of 1−10 s.

3.2.3 Fluorescence correlation spectroscopy

Fluorescence correlation spectroscopy (FCS) has provided evidence of anomalous diffusion of membrane proteins in live cells for more than a decade (Weiss, Hashimoto, & Nilsson, 2003). FCS yields local measurements with high temporal resolution and thus, it is an attractive method for the study of membrane organization but the reliable analysis of the modes of motion is challenging. Detailed reviews on its application to the study of diffusion in biological membranes are available (Chiantia, Ries, & Schwille, 2009; He & Marguet, 2011). Wawrezinieck, Rigneault, Marguet, and Lenne (2005) proposed an FCS analysis at multiple spatial scales, by varying the spot size, to study membrane organization and detect transient confinement within microdomains. Employing this analysis, it was observed that the motion of transferrin receptors is hindered by a meshwork, such as that sketched in Figure 4(A) (Lenne et al., 2006). However, the complex interplay of different mechanisms simultaneously affecting protein motion makes it difficult to characterize the effect of the cortical cytoskeleton on protein diffusion. Heinemann et al. (2013) studied the effect of membrane-bound actin on the lateral diffusion of proteins and lipids using an interesting in vitro system where biotinylated actin filaments were coupled to a free standing membrane, mimicking the cortical actin cytoskeleton. It was found that modulation of diffusion depended on the type and size of diffusing species and it was directly correlated to the bound actin density.

3.3 Macromolecular crowding and viscoelastic effects

The presence of mobile obstacles in the plasma membrane decreases the available space upon which molecules can move freely and as a consequence, the diffusion coefficient decreases. This intuitive effect is well established through both numerical simulations (Saxton, 1987) and experiments in reconstituted model membranes (Peters & Cherry, 1982; Vaz, Goodsaidzalduondo, & Jacobson, 1984). Thus, molecular crowding hinders mobility by reducing the diffusion coefficient, but the full extent of its effects on anomalous diffusion in membranes is not well understood (Banks & Fradin, 2005). The picture is clearer in three dimensions where macromolecular crowding has been observed to introduce viscoelasticity and subdiffusion (Banks & Fradin, 2005; Weiss, Guigas, & Kalla, 2007). As mentioned above, diffusion in a viscoelastic medium yields anomalous diffusion because the perturbations

induced by a molecule on its surroundings display a slow relaxation to its new configuration. Thus, a memory effect pushes particles back to their past locations. Up to date, evidence for two-dimensional viscoelastic effects in live cells is indirect and further work is needed to quantify the implications of viscoelasticity on the diffusion of membrane proteins. In particular, better experiments need to be designed to probe the impact of the mechanical properties of the membrane on the diffusion pattern.

Some of the most clear experimental evidence for the effect of protein crowding on lateral diffusion was obtained by Horton, Hofling, Radler, and Franosch (2010) in synthetic model membrane systems with an adjustable degree of crowding. The study of protein anomalous diffusion was performed with FCS as a function of avidin content. Avidin was bound to biotinylated-anchored lipids and, in order to record an FCS signal, a fraction of the avidin was fluorescently labeled. For intermediate and high protein crowding levels, anomalous diffusion was observed for the whole measurement range, between 0.1 and 100 ms, in agreement with molecular dynamics simulations (Javanainen et al., 2013). The onset of anomalous dynamics due to molecular crowding was measured by varying the fraction of lipids that contained biotin anchors and thus, different protein concentrations were attained. Anomalous diffusion takes place at 0.05% anchors (1:2000 anchor-to-lipid ratio) and the anomalous diffusion exponent decreases monotonically as the anchor concentration increases from 0.05% to 10%.

The evidence for viscoelasticity in cell membranes comes from mechanical measurements. Several types of mechanical tests are performed on cellular environments showing that the plasma membrane is viscoelastic. These measurements typically employ atomic force microscopy (AFM), traction force spectroscopy, and tether formation by optical or magnetic tweezers. Traction force microscopy (TFM) is a method for probing the local forces exerted by adherent cells on a substrate by visualization of substrate deformations. Typically fluorescent beads (Beningo & Wang, 2002) or micropatterned fluorescent spots (Polio, Rothenberg, Stamenović, & Smith, 2012) are embedded in a polyacrylic acid (PAA) matrix and their displacement can be directly observed. Then, the mechanical deformation of the PAA substrate is inferred. TFM measurements show that the cytoskeleton exhibits local viscoelastic properties (Kumar et al., 2006). Given that cytoskeleton fibers confer tension to the plasma membrane, we expect the membrane to display viscoelastic properties as well. More direct evidence for the viscoelasticity of the plasma membrane is obtained via tether formation (Ermilov, Murdock,

Qian, Brownell, & Anvari, 2007; Jauffred, Callisen, & Oddershede, 2007; Schmitz, Benoit, & Gottschalk, 2008). In tether formation experiments, a functionalized microsphere is attached to the cell membrane and then it is pulled away using optical or magnetic tweezers. Pulling can be performed at different velocities and the membrane tension is measured. Alternatively, the membrane viscoelasticity can be probed by AFM. The advantages of AFM lie in their high spatiotemporal resolution and the ability to probe local forces (Bao & Suresh, 2003). AFM data provide clear evidence for viscoelasticity over broad length- and timescales (Cartagena & Raman, 2014). Measurements show that bacterial cell walls are also viscoelastic. Vadillo-Rodriguez and Dutcher (2011) review the viscoelastic properties of bacterial envelopes in terms of both experiments and modeling. Even though evidence for viscoelasticity of the cell membranes is irrefutable, the detailed mechanisms causing viscoelasticity are still poorly understood. In particular, deformations of the cytoskeleton are known to cause viscoelastic properties, but its impact on protein diffusion can be very different from those caused by protein crowding.

3.4 Transient binding—seconds to minutes

Transient immobilizations with power-law distributed sojourn times lead rich physical properties including anomalous diffusion, aging, and weak *ergodicity breaking*. Molecules in the plasma membrane can interact with other membrane or cytoplasmic complexes in such a way that they immobilize during the time they are bound to immobile complexes. We have shown that in mammalian cells, the voltage-gated potassium channels Kv2.1 and Kv1.4 immobilize in the plasma membrane with sojourn times distributed according to power laws (Weigel, Simon, et al., 2011). Further, these interactions introduce aging in the protein trajectories because the longer the measurement time, the higher the chances of finding a more stable trap with longer binding times (Figure 5(A)). Thus, the mobile fraction time of each trajectory decreases when the observation time increases and, in turn, the apparent diffusion coefficient decreases as well. A distribution of sojourn times $\psi(\tau) \sim \tau^{-(1+\alpha)}$ yields an ensemble- and time-averaged mean squared displacement that scales as $\langle \overline{\delta^2} \rangle \sim T^{-(1-\alpha)}$, where T is the experimental time. For Kv2.1, $\alpha = 0.9$ according to the scaling behavior of both the measured sojourn time distribution and the aging of the MSD (Figure 5(A) and (B)). This behavior is found in timescales ranging from seconds to minutes. Different Kv channels exhibit α values between 0.8 and 0.9.

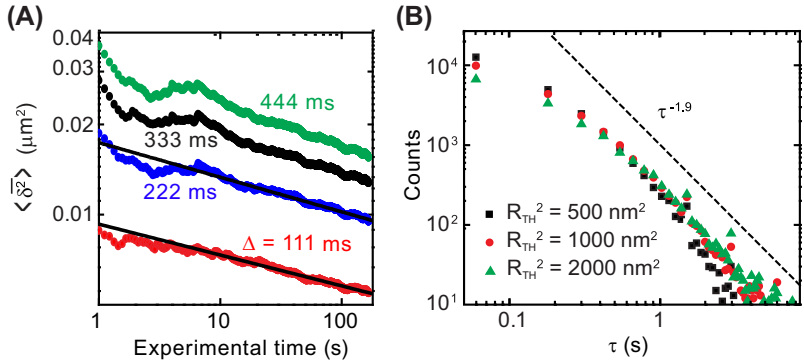

Figure 5 The ion channel Kv2.1 exhibits features of a heavy-tailed CTRW (Weigel, Simon, et al., 2011). (A) Aging. The ensemble average of the temporal mean square displacement (MSD) ($\langle\overline{\delta^2}\rangle$) is shown as a function of experimental time for four different lag times, namely $\Delta = 111$, 222, 333, and 444 ms. The averaged MSD depends on the experimental time with $\langle\overline{\delta^2}\rangle \sim 1/T^{0.1}$. Following Eqn (15), this observation is consistent with a CTRW with $\alpha = 0.9$. (B) Distribution of immobilization times of the Kv2.1 channel. Immobilizations are identified as a particle being temporarily confined within a radius R_{TH} and analyses employing different thresholds are shown. The distribution exhibits a power-law dependence $\psi(\tau) \sim \tau^{-(1+\alpha)}$, also with $\alpha = 0.9$. (See color plate)

Systems with power-law sojourn times exhibit weak ergodicity breaking, that is, the time average does not converge to the ensemble average because the time averages remain a random variable in the long time limit (Bel & Barkai, 2005; He et al., 2008; Lubelski et al., 2008). The measurements of Kv channels show that the MSD when averaged over time exhibits a large scatter, i.e., it displays a very broad distribution, but the MSD averaged over an ensemble of molecules does not, i.e., they have a narrow distribution (Weigel, Simon, et al., 2011). Similar observations have been made for three-dimensional diffusion in cellular environments for lipid (Jeon et al., 2011) and insulin granules (Tabei et al., 2013). Other three-dimensional diffusion measurements have shown large scattering of the temporal MSD. These include RNA molecules in bacteria (Golding & Cox, 2006) and telomeres in the nucleus of eukaryotic cells (Bronstein et al., 2009), but rigorous analyses show that this motion cannot be described by a CTRW and an fBM is more suitable (Kepten et al., 2011; Magdziarz et al., 2009).

Recent studies have elucidated the mechanism by which power-law sojourn times are observed in the immobilization of Kv channels on the plasma membrane (Weigel et al., 2013). It was found that channels immobilize when they bind to CCP in a catch-and-release manner. Clathrin structures are responsible for the internalization of receptors from the plasma

membrane (Doherty & McMahon, 2009; Edeling, Smith, & Owen, 2006). CCPs nucleate at locations next to junctions between the plasma membrane and the endoplasmic reticulum (Fox et al., 2013) and they grow as they mature and become ready for internalization. CCPs bind cargo such as Kv channels via interactions with an adaptor meshwork on the clathrin coat (Robinson, 2004). As a CCP grows, more adaptors become available for binding cargo and the escape rate from an individual coat decreases (Loerke, Mettlen, Schmid, & Danuser, 2011; Weigel et al., 2013). Thus the process is not Markovian because the longer a cargo molecule sits on a CCP, the smaller its probability of escape. As a result, sojourn times within CCPs have a power-law component that induces aging and anomalous diffusion. This type of motion is modeled as a heavy-tailed CTRW (see Section 2.2.1).

Different receptors have also been observed to display a similar catch-and-release behavior on CCPs as Kv channels (Torreno-Pina et al., 2014). Specifically, it was observed that transmembrane glycoprotein dendritic cell-specific intercellular adhesion molecule 3-grabbing nonintegrin (DC-SIGN) interacts with CCPs in a dynamic way. DC-SIGN interactions with clathrin coats appear to be tuned by the attachment of glycans. Interestingly, Torreno-Pina et al. (2014) showed that CCP-cargo interactions can be regulated by the localization of molecules to the vicinity of CCP regions. Specifically DC-SIGN localizes to nanodomains close to CCPs enhancing the probability of successful internalization. Therefore, antipersistent subdiffusion mechanisms, such as compartmentalization of the plasma membrane and fBM, enhance the interactions of cargo with CCP by maintaining reactants near their reaction centers. These observations are relevant for both Kv channels (Weigel, Simon, et al., 2011) and DC-SIGN (Torreno-Pina et al., 2014), where the exploration in the surrounding of CCPs is compact. We believe this is an important physiological role of anomalous diffusion on the plasma membrane and on the cell organization in general. Peculiarly, transient binding is not the sole mechanism for subdiffusion in either Kv channels or DC-SIGN. For the case of DC-SIGN, they are observed to exhibit clustering and confinement within nanoscale domains (de Bakker et al., 2007; Cambi et al., 2004). On the other hand, Kv channels are seen to exhibit anticorrelated type of subdiffusion while they are in the mobile phase and this subdiffusion persists for long times (Weigel, Simon, et al., 2011).

One key aspect of anomalous diffusion induced by transient immobilizations is that sojourn times exhibit very broad distributions. For

interactions with CCP, this phenomenon is enhanced by the heterogeneity of clathrin-coated pits, which leads to a broad distribution in CCP dwell times on the plasma membrane. It was shown that for a single cell, different populations of CCP exist: short-lived populations correspond to abortive events that do not end in internalization and long-lived events lasting up to several minutes involve the production of a vesicle (Loerke et al., 2011, 2009; Mettlen, Loerke, Yarar, Danuser, & Schmid, 2010). In a recent work, it was shown that the distribution of dwell times of CCPs depends on the cargo molecules that bind to it (Flores-Otero et al., 2014). Flores-Otero et al. (2014) studied the signaling cascade of specific GPCR, one of the most important signal transduction systems in cell biology and pharmacology. It was found that different agonists bound to the same GPCR can introduce significant changes to CCP dwell times. Therefore, many sources lead to heterogeneity in the time that molecules remain bound to CCP. Importantly, longer CCP dwell times enhance G protein signaling; thus, the ability for molecules to remain immobilized during long times, such as those modeled with power-law distributions, has direct physiological implications.

3.5 Membrane heterogeneities

As proteins explore different microdomains on the cell surface, their diffusion coefficient depends on the local environment. For example, single-particle tracking revealed that glycine receptors alternate between diffusive and confined states due to interactions with gephyrin, which are believed to regulate glycine receptor clustering during the formation of synapses between neurons (Meier et al., 2001). As discussed above, a heterogeneous diffusion landscape can lead to complex dynamics involving anomalous diffusion, aging, and weak ergodicity breaking (Cherstvy et al., 2013; Massignan et al., 2014). These nontrivial aspects of diffusion in a heterogeneous landscape resemble a system with a broad distribution of energetic traps where transient immobilizations due to reversible chemical binding can be modeled by a CTRW (Condamin, Tejedor, Voituriez, Benichou, & Klafter, 2008; Klafter & Sokolov, 2011; Weigel, Simon, et al., 2011; Weigel et al., 2013). Notably, it was recently reported that the motion of DC-SIGN in the plasma membrane exhibits anomalous diffusion and weak ergodicity breaking (Manzo et al., 2015). Nevertheless, it is shown that in this case, ergodicity breaking arises from heterogeneous diffusivity such as that described by patches of random sizes (Massignan et al., 2014), rather than transient immobilizations.

3.5.1 Single-particle tracking—study of diffusion and energy landscapes

Several tools have been recently developed to probe diffusivity landscapes with high spatial resolution (Sibarita, 2014). These nanoscopy techniques comprise natural adaptations of single-particle tracking and superresolution imaging. Single-particle tracking photoactivated localization microscopy (sptPALM) (Manley et al., 2008) uses photoactivatable fluorescence proteins suitable for superresolution imaging (Betzig et al., 2006). In sptPALM, a small subset of the fluorescence proteins are photoactivated and imaged until they photobleach. By introducing a photoactivation violet laser beam, a steady-state density of photoactivated molecules are maintained on the cell surface and these molecules can be tracked (Manley et al., 2008). Short traces are typically obtained but it is possible to map the surface of the cell with very high trajectory densities. Alternatively, instead of employing photoactivatable proteins, it is possible to tag molecules with fluorescently labeled antibodies. Here, antibodies rapidly diffuse in solution and only when they are captured at the cell surface they slow down to a level that enables their individual detection (Giannone et al., 2010). Freely diffusing antibodies move too fast and they are only seen as a dim background. When an antibody binds to the target molecule, it is tracked until it either photobleaches or it dissociates from the cell surface. This technique has been termed universal point accumulation for imaging in nanoscale topographies (uPAINT). It provides single molecule trajectories of up to tens of seconds at densities up to 120 μm^{-2} (Giannone et al., 2010). A completely different approach to high-density tracking was developed by the Lidke group, by taking advantage of the different spectral properties of different QDs (Cutler et al., 2013). Individual QDs are identified by their spectral properties allowing the simultaneous tracking of multiple particles within a diffraction-limited spot. The advantage of this tool is that high densities are possible while individual trajectories can be traced for minutes due to the nonbleaching properties of QDs.

Using uPAINT, diffusion heterogeneities were analyzed and a superresolved two-dimensional spatial map of the displacements was built by Giannone et al. (2010). A correlation diagram of glycosylphosphatidylinisotol (GPI)-anchored protein displacement steps and surface density shows that molecules accumulate in micrometer-sized domains where they exhibit slower diffusivity. A similar analysis of a model transmembrane protein, TM-6His, shows reduced mobility at the cell edges of fibroblasts (Giannone et al., 2010). AMPA receptors have also been found to exhibit reduced

mobility in regions of receptor accumulation such as synaptic sites (Giannone et al., 2010; Tardin, Cognet, Bats, Lounis, & Choquet, 2003). In order to accurately map both the diffusion and energy landscapes on the cell surface, a statistical approach using Bayesian inference was developed by the Masson group (Masson et al., 2009; Turkcan, Alexandrou, & Masson, 2012). This method was originally developed to analyze the motion of confined molecules and later expanded to a complete description of the heterogeneous diffusivity and energy landscapes (Masson et al., 2014). The starting point of this analysis is single-particle tracking data obtained by either uPAINT or sptPALM. It is found that diffusion maps exhibit large fluctuations at submicrometer length scales for different membrane proteins including glycine receptors (Masson et al., 2014), AMPA receptors (Hoze et al., 2012), and voltage-gated sodium channels (Akin et al., 2014).

3.5.2 Fluorescence correlation spectroscopy—clustering and lipid rafts

Membrane heterogeneities have been also recently studied with imaging FCS techniques such as imaging total internal reflection FCS (ITIR-FCS) (Kannan et al., 2007; Singh & Wohland, 2014). Imaging FCS is a multiplexed measurement that uses a fast camera to enable the simultaneous calculation of temporal correlations at each pixel. Di Rienzo, Gratton, Beltram, and Cardarelli (2013) analyzed the full space—time correlation function to probe population behavior in micrometer-sized plasma membrane regions and reconstructed the ensemble-averaged MSD for different lag times. With this approach the diffusion coefficient and confinement by the actin cytoskeleton were obtained for GFP-labeled transferrin receptors. Bag, Ali, Chauhan, Wohland, and Mishra (2013) used ITIR-FCS to study the dynamics of amylin-membrane interactions. Guo et al. extended this analysis by employing a Bayesian model selection and parameter estimation for resolving membrane heterogeneities and organization (Guo, Bag, Mishra, Wohland, & Bathe, 2014), a method originally developed for confocal FCS (Guo et al., 2012; He, Guo, & Bathe, 2012). The Bayesian ITIR-FCS approach was applied both to supported lipid bilayers and live cells, showing two-component phase separation in model membranes and the dynamic formation of amylin-induced domains in the plasma membrane of neuroblastoma cells (Guo et al., 2014).

A source of heterogeneity in the plasma membrane arises from the preferential aggregation between sphingolipids, sterols, and specific proteins. Therefore, dynamic complexes assemble in the form of isolated microdomains, termed lipid rafts, with different diffusion coefficient than the rest

of the plasma membrane (Lingwood & Simons, 2010; Simons & Ikonen, 1997; Simons & Sampaio, 2011). However, the direct observation of lipid rafts in live cells is often elusive due to their transient nature and their small sizes, typically in the range 5–200 nm. Direct observations of the transient trapping of sphingolipids and GPI-anchored proteins within nanodomains were enabled by combining FCS with stimulated emission depletion (STED) fluorescence microscopy (Eggeling et al., 2009; Mueller et al., 2011). STED is a superresolution technique where the probe volume is confined to a region not constrained by the diffraction limit and thus, it permits diffusion measurements at length scales relevant to lipid rafts with high temporal resolution (Kastrup, Blom, Eggeling, & Hell, 2005). Billaudeau et al. (2013) review the use of spot variation FCS for the investigation of the nanoscale organization of the plasma membrane. These experiments reveal molecular details showing that constrained diffusion is often caused by cholesterol-assisted molecular complexes. Further STED-FCS allows the determination of on- and off-rates as well as the domain size (Veronika Mueller et al., 2012).

4. CONCLUSIONS

Many membrane proteins display anomalous diffusion. The physical mechanism of subdiffusion and its timescale depends on the specific type of molecule. Generally, it is observed that molecules with large cytoplasmic domains are strongly affected by collisions with the actin cytoskeleton that affect their motion up to minutes. Small molecules or lipids show subdiffusion on smaller timescales. The exact range of timescales for these molecules is still under debate and, depending on the specific molecule, can be from microseconds to milliseconds.

The picture that arises from the plasma membrane is that of a highly complex environment where interactions between many players lead to intriguing emerging phenomena. Early attempts to classify the mechanisms of anomalous diffusion on the cell surface appear to have underestimated cellular complexity. Instead, a picture with different mechanisms coexisting seems to be more realistic, with these mechanisms displaying strong coupling between them in such a way that it is difficult to decompose them into individual simpler phenomena. Furthermore, the complexity of diffusion in live cells continues to inspire new modeling tools which are needed to understand fundamental biophysical processes.

ACKNOWLEDGMENTS

I thank Eli Barkai for carefully reading the manuscript and for many productive discussions. I also thank Liz Akin, Jenny Higgins, Sanaz Sadegh, Mike Tamkun, and Aubrey Weigel for useful discussions.

I acknowledge the support from the National Science Foundation under grant number 1401432.

REFERENCES

Aguet, F., Antonescu, C. N., Mettlen, M., Schmid, S. L., & Danuser, G. (2013). Advances in analysis of low signal-to-noise images link dynamin and AP2 to the functions of an endocytic checkpoint. *Developmental Cell, 26*(3), 279–291.

Akimoto, T., Yamamoto, E., Yasuoka, K., Hirano, Y., & Yasui, M. (2011). Non-Gaussian fluctuations resulting from power-law trapping in a lipid bilayer. *Physical Review Letters, 107*(17), 178103.

Akin, E. J., Brown, K., Sadegh, S., Weigel, A. V., Masson, J.-B., Krapf, D., et al. (2014). Single-particle tracking PALM of Nav1.6 in hippocampal neurons demonstrates unique subcellular diffusion landscapes. *Biophysical Journal, 106*(2), 36a.

Alberts, B., Johnson, A., Lewis, J., Raff, M., Roberts, K., & Walter, P. (2010). *Molecular biology of the cell.* New York: Garland Science.

Almeida, P. F. F., Vaz, W. L. C., & Thompson, T. E. (1992). Lateral diffusion in the liquid-phases of dimyristoylphosphatidylcholine cholesterol lipid bilayers: a free-volume analysis. *Biochemistry, 31*(29), 6739–6747.

Anderluh, A., Klotzsch, E., Ries, J., Reismann, A. W., Weber, S., Fölser, M., et al. (2014). Tracking single serotonin transporter molecules at the endoplasmic reticulum and plasma membrane. *Biophysical Journal, 106*(9), L33–L35.

Andrews, N. L., Lidke, K. A., Pfeiffer, J. R., Burns, A. R., Wilson, B. S., Oliver, J. M., et al. (2008). Actin restricts Fcepsilon RI diffusion and facilitates antigen-induced receptor immobilization. *Nature Cell Biology, 10*(8), 955–963.

Bag, N., Ali, A., Chauhan, V. S., Wohland, T., & Mishra, A. (2013). Membrane destabilization by monomeric hIAPP observed by imaging fluorescence correlation spectroscopy. *Chemical Communications, 49*(80), 9155–9157.

de Bakker, B. I., de Lange, F., Cambi, A., Korterik, J. P., van Dijk, E. M. H. P., van Hulst, N. F., et al. (2007). Nanoscale organization of the pathogen receptor DC-SIGN mapped by single-molecule high-resolution fluorescence microscopy. *ChemPhysChem, 8*(10), 1473–1480.

Banks, D. S., & Fradin, C. (2005). Anomalous diffusion of proteins due to molecular crowding. *Biophysical Journal, 89*(5), 2960–2971.

Bao, G., & Suresh, S. (2003). Cell and molecular mechanics of biological materials. *Nature Materials, 2*(11), 715–725.

Bel, G., & Barkai, E. (2005). Weak ergodicity breaking in the continuous-time random walk. *Physical Review Letters, 94*(24), 240602.

Ben-Avraham, D., & Havlin, S. (2000). *Diffusion and reactions in fractals and disordered systems.* Cambridge: Cambridge University Press.

Beningo, K. A., & Wang, Y. L. (2002). Flexible substrata for the detection of cellular traction forces. *Trends in Cell Biology, 12*(2), 79–84.

Bennett, V., & Gilligan, D. M. (1993). The spectrin-based membrane skeleton and micron-scale organization of the plasma membrane. *Annual Review of Cell Biology, 9*(1), 27–66.

Betzig, E., Patterson, G. H., Sougrat, R., Lindwasser, O. W., Olenych, S., Bonifacino, J. S., et al. (2006). Imaging intracellular fluorescent proteins at nanometer resolution. *Science, 313*(5793), 1642–1645.

Billaudeau, C., Mailfert, S., Trombik, T., Bertaux, N., Rouger, V., Hamon, Y., et al. (2013). Probing the plasma membrane organization in living cells by spot variation fluorescence correlation spectroscopy. *Methods in Enzymology, 519*, 277–302.

Blumen, A., Klafter, J., White, B. S., & Zumofen, G. (1984). Continuous-time random-walks on fractals. *Physical Review Letters, 53*(14), 1301–1304.

Bouchaud, J.-P., & Georges, A. (1990). Anomalous diffusion in disordered media: statistical mechanisms, models and physical applications. *Physics Reports, 195*(4), 127–293.

de Brabander, M., Nuydens, R., Ishihara, A., Holifield, B., Jacobson, K., & Geerts, H. (1991). Lateral diffusion and retrograde movements of individual cell-surface components on single motile cells observed with nanovid microscopy. *Journal of Cell Biology, 112*(1), 111–124.

Bronstein, I., Israel, Y., Kepten, E., Mai, S., Shav-Tal, Y., Barkai, E., et al. (2009). Transient anomalous diffusion of telomeres in the nucleus of mammalian cells. *Physical Review Letters, 103*(1), 018102.

Burnecki, K., Kepten, E., Janczura, J., Bronshtein, I., Garini, Y., & Weron, A. (2012). Universal algorithm for identification of fractional Brownian motion. A case of telomere subdiffusion. *Biophysical Journal, 103*(9), 1839–1847.

Burov, S., Jeon, J. H., Metzler, R., & Barkai, E. (2011). Single particle tracking in systems showing anomalous diffusion: the role of weak ergodicity breaking. *Physical Chemistry Chemical Physics, 13*(5), 1800–1812.

Cambi, A., de Lange, F., van Maarseveen, N. M., Nijhuis, M., Joosten, B., van Dijk, E. M., et al. (2004). Microdomains of the C-type lectin DC-SIGN are portals for virus entry into dendritic cells. *Journal of Cell Biology, 164*(1), 145–155.

Cartagena, A., & Raman, A. (2014). Local viscoelastic properties of live cells investigated using dynamic and quasi-static atomic force microscopy methods. *Biophysical Journal, 106*(5), 1033–1043.

Casuso, I., Khao, J., Chami, M., Paul-Gilloteaux, P., Husain, M., Duneau, J. P., et al. (2012). Characterization of the motion of membrane proteins using high-speed atomic force microscopy. *Nature Nanotechnology, 7*(8), 525–529.

Cherstvy, A. G., Chechkin, A. V., & Metzler, R. (2013). Anomalous diffusion and ergodicity breaking in heterogeneous diffusion processes. *New Journal of Physics, 15*, 083039.

Cherstvy, A. G., & Metzler, R. (2014). Nonergodicity, fluctuations, and criticality in heterogeneous diffusion processes. *Physical Review E, 90*(1), 012134.

Chiantia, S., Ries, J., & Schwille, P. (2009). Fluorescence correlation spectroscopy in membrane structure elucidation. *Biochimica et Biophysica Acta (BBA)-Biomembranes, 1788*(1), 225–233.

Chichili, G. R., & Rodgers, W. (2009). Cytoskeleton–membrane interactions in membrane raft structure. *Cellular and Molecular Life Sciences, 66*(14), 2319–2328.

Condamin, S., Tejedor, V., Voituriez, R., Benichou, O., & Klafter, J. (2008). Probing microscopic origins of confined subdiffusion by first-passage observables. *Proceedings of the National Academy of Sciences of the United States of America, 105*(15), 5675–5680.

Costantini, L. M., Fossati, M., Francolini, M., & Snapp, E. L. (2012). Assessing the tendency of fluorescent proteins to oligomerize under physiologic conditions. *Traffic, 13*(5), 643–649.

Cui-Wang, T., Hanus, C., Cui, T., Helton, T., Bourne, J., Watson, D., et al. (2012). Local zones of endoplasmic reticulum complexity confine cargo in neuronal dendrites. *Cell, 148*(1), 309–321.

Cunningham, C. C. (1995). Actin polymerization and intracellular solvent flow in cell surface blebbing. *Journal of Cell Biology, 129*(6), 1589–1599.

Cutler, P. J., Malik, M. D., Liu, S., Byars, J. M., Lidke, D. S., & Lidke, K. A. (2013). Multi-color quantum dot tracking using a high-speed hyperspectral line-scanning microscope. *PLoS One, 8*(5), e64320.

Deng, W. H., & Barkai, E. (2009). Ergodic properties of fractional Brownian-Langevin motion. *Physical Review E, 79*(1), 011112.

Deverall, M. A., Gindl, E., Sinner, E. K., Besir, H., Ruehe, J., Saxton, M. J., et al. (2005). Membrane lateral mobility obstructed by polymer-tethered lipids studied at the single molecule level. *Biophysical Journal, 88*(3), 1875–1886.

Di Rienzo, C., Gratton, E., Beltram, F., & Cardarelli, F. (2013). Fast spatiotemporal correlation spectroscopy to determine protein lateral diffusion laws in live cell membranes. *Proceedings of the National Academy of Sciences of the United States of America, 110*(30), 12307–12312.

Doherty, G. J., & McMahon, H. T. (2009). Mechanisms of endocytosis. *Annual Review of Biochemistry, 78*, 857–902.

Dupuy, A. D., & Engelman, D. M. (2008). Protein area occupancy at the center of the red blood cell membrane. *Proceedings of the National Academy of Sciences of the United States of America, 105*(8), 2848–2852.

Edeling, M. A., Smith, C., & Owen, D. (2006). Life of a clathrin coat: insights from clathrin and AP structures. *Nature Reviews Molecular Cell Biology, 7*(1), 32–44.

Edidin, M., Kuo, S. C., & Sheetz, M. P. (1991). Lateral movements of membrane-glycoproteins restricted by dynamic cytoplasmic barriers. *Science, 254*(5036), 1379–1382.

Edidin, M., Zuniga, M. C., & Sheetz, M. P. (1994). Truncation mutants define and locate cytoplasmic barriers to lateral mobility of membrane glycoproteins. *Proceedings of the National Academy of Sciences of the United States of America, 91*(8), 3378–3382.

Eggeling, C., Ringemann, C., Medda, R., Schwarzmann, G., Sandhoff, K., Polyakova, S., et al. (2009). Direct observation of the nanoscale dynamics of membrane lipids in a living cell. *Nature, 457*(7233), 1159–1162.

Einstein, A. (1905). The motion of elements suspended in static liquids as claimed in the molecular kinetic theory of heat. *Annalen Der Physik, 17*(8), 549–560.

Ermilov, S. A., Murdock, D. R., Qian, F., Brownell, W. E., & Anvari, B. (2007). Studies of plasma membrane mechanics and plasma membrane-cytoskeleton interactions using optical tweezers and fluorescence imaging. *Journal of Biomechanics, 40*(2), 476–480.

Ernst, D., Hellmann, M., Kohler, J., & Weiss, M. (2012). Fractional Brownian motion in crowded fluids. *Soft Matter, 8*(18), 4886–4889.

Feder, T. J., Brust-Mascher, I., Slattery, J. P., Baird, B., & Webb, W. W. (1996). Constrained diffusion or immobile fraction on cell surfaces: a new interpretation. *Biophysical Journal, 70*(6), 2767–2773.

Flores-Otero, J., Ahn, K. H., Delgado-Peraza, F., Mackie, K., Kendall, D. A., & Yudowski, G. A. (2014). Ligand-specific endocytic dwell times control functional selectivity of the cannabinoid receptor 1. *Nature Communications, 5*, 4589.

Fogedby, H. C. (1994). Langevin-equations for continuous-time Levy flights. *Physical Review E, 50*(2), 1657–1660.

Fox, P. D., Haberkorn, C. J., Weigel, A. V., Higgins, J. L., Akin, E. J., Kennedy, M. J., et al. (2013). Plasma membrane domains enriched in cortical endoplasmic reticulum function as membrane protein trafficking hubs. *Molecular Biology of the Cell, 24*(17), 2703–2713.

Fujiwara, T., Ritchie, K., Murakoshi, H., Jacobson, K., & Kusumi, A. (2002). Phospholipids undergo hop diffusion in compartmentalized cell membrane. *Journal of Cell Biology, 157*(6), 1071–1081.

Gal, N., Lechtman-Goldstein, D., & Weihs, D. (2013). Particle tracking in living cells: a review of the mean square displacement method and beyond. *Rheologica Acta, 52*(5), 425–443.

Giannone, G., Hosy, E., Levet, F., Constals, A., Schulze, K., Sobolevsky, A. I., et al. (2010). Dynamic superresolution imaging of endogenous proteins on living cells at ultra-high density. *Biophysical Journal, 99*(4), 1303–1310.

Golding, I., & Cox, E. C. (2006). Physical nature of bacterial cytoplasm. *Physical Review Letters, 96*(9), 098102.

Goychuk, I., Kharchenko, V. O., & Metzler, R. (2014). How molecular motors work in the crowded environment of living cells: coexistence and efficiency of normal and anomalous transport. *PLoS One, 9*(3), e91700.

Guigas, G., Kalla, C., & Weiss, M. (2007). The degree of macromolecular crowding in the cytoplasm and nucleoplasm of mammalian cells is conserved. *FEBS Letters, 581*(26), 5094–5098.

Guo, S.-M., Bag, N., Mishra, A., Wohland, T., & Bathe, M. (2014). Bayesian total internal reflection fluorescence correlation spectroscopy reveals hIAPP-induced plasma membrane domain organization in live cells. *Biophysical Journal, 106*(1), 190–200.

Guo, S.-M., He, J., Monnier, N., Sun, G., Wohland, T., & Bathe, M. (2012). Bayesian approach to the analysis of fluorescence correlation spectroscopy data II: application to simulated and in vitro data. *Analytical Chemistry, 84*(9), 3880–3888.

Havlin, S., & Ben-Avraham, D. (1987). Diffusion in disordered media. *Advances in Physics, 36*(6), 695–798.

He, Y., Burov, S., Metzler, R., & Barkai, E. (2008). Random time-scale invariant diffusion and transport coefficients. *Physical Review Letters, 101*(5), 058101.

He, J., Guo, S.-M., & Bathe, M. (2012). Bayesian approach to the analysis of fluorescence correlation spectroscopy data I: theory. *Analytical Chemistry, 84*(9), 3871–3879.

He, H.-T., & Marguet, D. (2011). Detecting nanodomains in living cell membrane by fluorescence correlation spectroscopy. *Annual Review of Physical Chemistry, 62*, 417–436.

Heinemann, F., Vogel, S. K., & Schwille, P. (2013). Lateral membrane diffusion modulated by a minimal actin cortex. *Biophysical Journal, 104*(7), 1465–1475.

Höfling, F., & Franosch, T. (2013). Anomalous transport in the crowded world of biological cells. *Reports on Progress in Physics, 76*(4), 046602.

Horton, M. R., Hofling, F., Radler, J. O., & Franosch, T. (2010). Development of anomalous diffusion among crowding proteins. *Soft Matter, 6*(12), 2648–2656.

Hoze, N., Nair, D., Hosy, E., Sieben, C., Manley, S., Herrmann, A., et al. (2012). Heterogeneity of AMPA receptor trafficking and molecular interactions revealed by superresolution analysis of live cell imaging. *Proceedings of the National Academy of Sciences of the United States of America, 109*(42), 17052–17057.

James, P. S., Hennessy, C., Berge, T., & Jones, R. (2004). Compartmentalisation of the sperm plasma membrane: a FRAP, FLIP and SPFI analysis of putative diffusion barriers on the sperm head. *Journal of Cell Science, 117*(26), 6485–6495.

Jauffred, L., Callisen, T. H., & Oddershede, L. B. (2007). Visco-elastic membrane tethers extracted from *Escherichia coli* by optical tweezers. *Biophysical Journal, 93*(11), 4068–4075.

Javanainen, M., Hammaren, H., Monticelli, L., Jeon, J. H., Miettinen, M. S., Martinez-Seara, H., et al. (2013). Anomalous and normal diffusion of proteins and lipids in crowded lipid membranes. *Faraday Discussions, 161*, 397–417.

Jeon, J. H., Monne, H. M. S., Javanainen, M., & Metzler, R. (2012). Anomalous diffusion of phospholipids and cholesterols in a lipid bilayer and its origins. *Physical Review Letters, 109*(18), 188103.

Jeon, J. H., Tejedor, V., Burov, S., Barkai, E., Selhuber-Unkel, C., Berg-Sorensen, K., et al. (2011). In vivo anomalous diffusion and weak ergodicity breaking of lipid granules. *Physical Review Letters, 106*(4), 048103.

Jiang, H., English, B. P., Hazan, R. B., Wu, P., & Ovryn, B. (2015). Tracking surface glycans on live cancer cells with single-molecule sensitivity. *Angewandte Chemie International Edition, 54*(6), 1765–1769.

Kannan, B., Guo, L., Sudhaharan, T., Ahmed, S., Maruyama, I., & Wohland, T. (2007). Spatially resolved total internal reflection fluorescence correlation microscopy using an electron multiplying charge-coupled device camera. *Analytical Chemistry, 79*(12), 4463–4470.

Kastrup, L., Blom, H., Eggeling, C., & Hell, S. W. (2005). Fluorescence fluctuation spectroscopy in subdiffraction focal volumes. *Physical Review Letters, 94*(17), 178104.

Kepten, E., Bronshtein, I., & Garini, Y. (2011). Ergodicity convergence test suggests telomere motion obeys fractional dynamics. *Physical Review E, 83*(4), 041919.

Klafter, J., Blumen, A., & Zumofen, G. (1984). Fractal behavior in trapping and reaction: a random-walk study. *Journal of Statistical Physics, 36*(5–6), 561–577.

Klafter, J., & Sokolov, I. M. (2005). Anomalous diffusion spreads its wings. *Physics World, 18*(8), 29–32.

Klafter, J., & Sokolov, I. M. (2011). *First steps in random walks: From tools to applications*. New York: Oxford University Press.

Kumar, S., Maxwell, I. Z., Heisterkamp, A., Polte, T. R., Lele, T. P., Salanga, M., et al. (2006). Viscoelastic retraction of single living stress fibers and its impact on cell shape, cytoskeletal organization, and extracellular matrix mechanics. *Biophysical Journal, 90*(10), 3762–3773.

Kuo, H.-H. (2006). *Introduction to stochastic integration*. New York: Springer.

Kusumi, A., Fujiwara, T. K., Chadda, R., Xie, M., Tsunoyama, T. A., Kalay, Z., et al. (2012). Dynamic organizing principles of the plasma membrane that regulate signal transduction: commemorating the fortieth anniversary of Singer and Nicolson's fluid-mosaic model. *Annual Review of Cell and Developmental Biology, 28*, 215–250.

Kusumi, A., Nakada, C., Ritchie, K., Murase, K., Suzuki, K., Murakoshi, H., et al. (2005). Paradigm shift of the plasma membrane concept from the two-dimensional continuum fluid to the partitioned fluid: high-speed single-molecule tracking of membrane molecules. *Annual Review of Biophysics and Biomolecular Structure, 34*, 351–378.

Kusumi, A., & Sako, Y. (1996). Cell surface organization by the membrane skeleton. *Current Opinion in Cell Biology, 8*(4), 566–574.

Lenne, P. F., Wawrezinieck, L., Conchonaud, F., Wurtz, O., Boned, A., Guo, X. J., et al. (2006). Dynamic molecular confinement in the plasma membrane by microdomains and the cytoskeleton meshwork. *EMBO Journal, 25*(14), 3245–3256.

Lingwood, D., & Simons, K. (2010). Lipid rafts as a membrane-organizing principle. *Science, 327*(5961), 46–50.

Lodish, H., Berk, A., Kaiser, C. A., Krieger, M., Scott, M. P., Bretscher, A., et al. (2007). *Molecular cell biology* (6th ed.). New York: W. H. Freeman.

Loerke, D., Mettlen, M., Schmid, S. L., & Danuser, G. (2011). Measuring the hierarchy of molecular events during clathrin-mediated endocytosis. *Traffic, 12*(7), 815–825.

Loerke, D., Mettlen, M., Yarar, D., Jaqaman, K., Jaqaman, H., Danuser, G., et al. (2009). Cargo and dynamin regulate clathrin-coated pit maturation. *PLoS Biology, 7*(3), 628–639.

Lubelski, A., Sokolov, I. M., & Klafter, J. (2008). Nonergodicity mimics inhomogeneity in single particle tracking. *Physical Review Letters, 100*(25), 250602.

Luna, E. J., & Hitt, A. L. (1992). Cytoskeleton–plasma membrane interactions. *Science, 258*(5084), 955–964.

Magdziarz, M., Weron, A., Burnecki, K., & Klafter, J. (2009). Fractional Brownian motion versus the continuous-time random walk: a simple test for subdiffusive dynamics. *Physical Review Letters, 103*(18), 180602.

Mandelbrot, B., & Van Ness, J. W. (1968). Fractional Brownian motions fractional noises and applications. *SIAM Review, 10*(4), 422–437.

Manley, S., Gillette, J. M., Patterson, G. H., Shroff, H., Hess, H. F., Betzig, E., et al. (2008). High-density mapping of single-molecule trajectories with photoactivated localization microscopy. *Nature Methods, 5*(2), 155–157.

Manzo, C., Torreno-Pina, J. A., Massignan, P., Lapeyre, G. J., Lewenstein, M., & Garcia Parajo, M. F. (2015). Weak ergodicity breaking of receptor motion in living cells stemming from random diffusivity. *Physical Review X, 5*(1), 011021.

Marguet, D., Lenne, P. F., Rigneault, H., & He, H. T. (2006). Dynamics in the plasma membrane: how to combine fluidity and order. *EMBO Journal, 25*(15), 3446–3457.

Mason, T. G., & Weitz, D. A. (1995). Optical measurements of frequency-dependent linear viscoelastic moduli of complex fluids. *Physical Review Letters, 74*(7), 1250–1253.

Massignan, P., Manzo, C., Torreno-Pina, J. A., Garcia-Parajo, M. F., Lewenstein, M., & Lapeyre, G. J. (2014). Nonergodic subdiffusion from Brownian motion in an inhomogeneous medium. *Physical Review Letters, 112*(15), 150603.

Masson, J. B., Casanova, D., Turkcan, S., Voisinne, G., Popoff, M. R., Vergassola, M., et al. (2009). Inferring maps of forces inside cell membrane microdomains. *Physical Review Letters, 102*(4), 048103.

Masson, J. B., Dionne, P., Salvatico, C., Renner, M., Specht, C. G., Triller, A., et al. (2014). Mapping the energy and diffusion landscapes of membrane proteins at the cell surface using high-density single-molecule imaging and Bayesian inference: application to the multiscale dynamics of glycine receptors in the neuronal membrane. *Biophysical Journal, 106*(1), 74–83.

Meier, J., Vannier, C., Serge, A., Triller, A., & Choquet, D. (2001). Fast and reversible trapping of surface glycine receptors by gephyrin. *Nature Neuroscience, 4*(3), 253–260.

Meroz, Y., Sokolov, I. M., & Klafter, J. (2010). Subdiffusion of mixed origins: when ergodicity and nonergodicity coexist. *Physical Review E, 81*(1), 010101(R).

Mettlen, M., Loerke, D., Yarar, D., Danuser, G., & Schmid, S. L. (2010). Cargo- and adaptor-specific mechanisms regulate clathrin-mediated endocytosis. *Journal of Cell Biology, 188*(6), 919–933.

Metzler, R., Jeon, J.-H., Cherstvy, A. G., & Barkai, E. (2014). Anomalous diffusion models and their properties: non-stationarity, non-ergodicity, and ageing at the centenary of single particle tracking. *Physical Chemistry Chemical Physics, 16*(44), 24128–24164. http://dx.doi.org/10.1039/C4CP03465A.

Metzler, R., & Klafter, J. (2000). The random walk's guide to anomalous diffusion: a fractional dynamics approach. *Physics Reports, 339*(1), 1–77.

Michalet, X., Pinaud, F. F., Bentolila, L. A., Tsay, J. M., Doose, S., Li, J. J., et al. (2005). Quantum dots for live cells, in vivo imaging, and diagnostics. *Science, 307*(5709), 538–544.

Mueller, V., Honigmann, A., Ringemann, C., Medda, R., Schwarzmann, G., & Eggeling, C. (2012). FCS in STED microscopy: studying the nanoscale of lipid membrane dynamics. *Methods in Enzymology, 519*, 1–38.

Mueller, V., Ringemann, C., Honigmann, A., Schwarzmann, G., Medda, R., Leutenegger, M., et al. (2011). STED nanoscopy reveals molecular details of cholesterol-and cytoskeleton-modulated lipid interactions in living cells. *Biophysical Journal, 101*(7), 1651–1660.

Murase, K., Fujiwara, T., Umemura, Y., Suzuki, K., Iino, R., Yamashita, H., et al. (2004). Ultrafine membrane compartments for molecular diffusion as revealed by single molecule techniques. *Biophysical Journal, 86*(6), 4075–4093.

Nakada, C., Ritchie, K., Oba, Y., Nakamura, M., Hotta, Y., Iino, R., et al. (2003). Accumulation of anchored proteins forms membrane diffusion barriers during neuronal polarization. *Nature Cell Biology, 5*(7), 626–632.

Notelaers, K., Rocha, S., Paesen, R., Smisdom, N., De Clercq, B., Meier, J. C., et al. (2014). Analysis of alpha 3 GlyR single particle tracking in the cell membrane. *Biochimica Et Biophysica Acta-Molecular Cell Research, 1843*(3), 544–553.

Notelaers, K., Smisdom, N., Rocha, S., Janssen, D., Meier, J. C., Rigo, J. M., et al. (2012). Ensemble and single particle fluorimetric techniques in concerted action to study the diffusion and aggregation of the glycine receptor alpha 3 isoforms in the cell plasma membrane. *Biochimica Et Biophysica Acta-Biomembranes, 1818*(12), 3131–3140.

Peebles, P. Z. (1987). *Probability, random variables, and random signal principles* (3rd ed.). New York: McGraw-Hill.

Peters, R., & Cherry, R. J. (1982). Lateral and rotational diffusion of bacteriorhodopsin in lipid bilayers - experimental test of the Saffman-Delbruck equations. *Proceedings of the National Academy of Sciences of the United States of America, 79*(14), 4317–4321.

Pinaud, F., Clarke, S., Sittner, A., & Dahan, M. (2010). Probing cellular events, one quantum dot at a time. *Nature Methods, 7*(4), 275–285.

Polio, S. R., Rothenberg, K. E., Stamenović, D., & Smith, M. L. (2012). A micropatterning and image processing approach to simplify measurement of cellular traction forces. *Acta Biomaterialia, 8*(1), 82–88.

Ritchie, K., Iino, R., Fujiwara, T., Murase, K., & Kusumi, A. (2003). The fence and picket structure of the plasma membrane of live cells as revealed by single molecule techniques (review). *Molecular Membrane Biology, 20*(1), 13–18.

Robinson, M. S. (2004). Adaptable adaptors for coated vesicles. *Trends in Cell Biology, 14*(4), 167–174.

Sako, Y., & Kusumi, A. (1995). Barriers for lateral diffusion of transferrin receptor in the plasma membrane as characterized by receptor dragging by laser tweezers: fence versus tether. *Journal of Cell Biology, 129*(6), 1559–1574.

Saxton, M. J. (1987). Lateral diffusion in an archipelago. The effect of mobile obstacles. *Biophysical Journal, 52*(6), 989–997.

Saxton, M. J. (1994). Anomalous diffusion due to obstacles: a Monte-Carlo study. *Biophysical Journal, 66*(2), 394–401.

Saxton, M. J. (1996). Anomalous diffusion due to binding: a Monte Carlo study. *Biophysical Journal, 70*(3), 1250–1262.

Saxton, M. J., & Jacobson, K. (1997). Single-particle tracking: applications to membrane dynamics. *Annual Review of Biophysics and Biomolecular Structure, 26*, 373–399.

Schaaf, M. J. M., Koopmans, W. J. A., Meckel, T., van Noort, J., Snaar-Jagalska, B. E., Schmidt, T. S., et al. (2009). Single-molecule microscopy reveals membrane microdomain organization of cells in a living vertebrate. *Biophysical Journal, 97*(4), 1206–1214.

Scher, H., & Montroll, E. W. (1975). Anomalous transit-time dispersion in amorphous solids. *Physical Review B, 12*(6), 2455–2477.

Scher, H., Shlesinger, M. F., & Bendler, J. T. (1991). Time-scale invariance in transport and relaxation. *Physics Today, 44*(1), 26–34.

Schmitz, J., Benoit, M., & Gottschalk, K. E. (2008). The viscoelasticity of membrane tethers and its importance for cell adhesion. *Biophysical Journal, 95*(3), 1448–1459.

Sebastian, K. L. (1995). Path-integral representation for fractional Brownian-motion. *Journal of Physics. A: Mathematical and General, 28*(15), 4305–4311.

Serge, A., Bertaux, N., Rigneault, H., & Marguet, D. (2008). Dynamic multiple-target tracing to probe spatiotemporal cartography of cell membranes. *Nature Methods, 5*(8), 687–694.

Sheetz, M. P. (1983). Membrane skeletal dynamics: role in modulation of red-cell deformability, mobility of transmembrane proteins, and shape. *Seminars in Hematology, 20*(3), 175–188.

Sheetz, M. P., Turney, S., Qian, H., & Elson, E. L. (1989). Nanometer-level analysis demonstrates that lipid flow does not drive membrane glycoprotein movements. *Nature, 340*(6231), 284–288.

Sibarita, J. B. (2014). High-density single-particle tracking: quantifying molecule organization and dynamics at the nanoscale. *Histochemistry and Cell Biology, 141*(6), 587–595.

Simons, K., & Ikonen, E. (1997). Functional rafts in cell membranes. *Nature, 387*(6633), 569–572.

Simons, K., & Sampaio, J. L. (2011). Membrane organization and lipid rafts. *Cold Spring Harbor Perspectives in Biology, 3*(10), a004697.

Singh, A. P., & Wohland, T. (2014). Applications of imaging fluorescence correlation spectroscopy. *Current Opinion in Chemical Biology, 20*, 29–35.

Smith, P. R., Morrison, I. E. G., Wilson, K. M., Fernandez, N., & Cherry, R. J. (1999). Anomalous diffusion of major histocompatibility complex class I molecules on HeLa cells determined by single particle tracking. *Biophysical Journal, 76*(6), 3331–3344.

Snapp, E. L., Hegde, R. S., Francolini, M., Lombardo, F., Colombo, S., Pedrazzini, E., et al. (2003). Formation of stacked ER cisternae by low affinity protein interactions. *Journal of Cell Biology, 163*(2), 257–269.

Sokolov, I. M., & Klafter, J. (2005). From diffusion to anomalous diffusion: a century after Einstein's Brownian motion. *Chaos, 15*(2), 026103.

Suzuki, K., Ritchie, K., Kajikawa, E., Fujiwara, T., & Kusumi, A. (2005). Rapid hop diffusion of a G-protein-coupled receptor in the plasma membrane as revealed by single-molecule techniques. *Biophysical Journal, 88*(5), 3659–3680.

Szymanski, J., & Weiss, M. (2009). Elucidating the origin of anomalous diffusion in crowded fluids. *Physical Review Letters, 103*(3), 038102.

Tabei, S. M. A., Burov, S., Kim, H. Y., Kuznetsov, A., Huynh, T., Jureller, J., et al. (2013). Intracellular transport of insulin granules is a subordinated random walk. *Proceedings of the National Academy of Sciences of the United States of America, 110*(13), 4911–4916.

Tank, D. W., Wu, E. S., & Webb, W. W. (1982). Enhanced molecular diffusibility in muscle membrane blebs: release of lateral constraints. *Journal of Cell Biology, 92*(1), 207–212.

Tardin, C., Cognet, L., Bats, C., Lounis, B., & Choquet, D. (2003). Direct imaging of lateral movements of AMPA receptors inside synapses. *EMBO Journal, 22*(18), 4656–4665.

Torreno-Pina, J. A., Castro, B. M., Manzo, C., Buschow, S. I., Cambi, A., & Garcia-Parajo, M. F. (2014). Enhanced receptor-clathrin interactions induced by N-glycan-mediated membrane micropatterning. *Proceedings of the National Academy of Sciences of the United States of America, 111*(30), 11037–11042.

Tsuji, A., & Ohnishi, S. (1986). Restriction of the lateral motion of band-3 in the erythrocyte-membrane by the cytoskeletal network: dependence on spectrin association state. *Biochemistry, 25*(20), 6133–6139.

Turkcan, S., Alexandrou, A., & Masson, J. B. (2012). A Bayesian inference scheme to extract diffusivity and potential fields from confined single-molecule trajectories. *Biophysical Journal, 102*(10), 2288–2298.

Vadillo-Rodriguez, V., & Dutcher, J. R. (2011). Viscoelasticity of the bacterial cell envelope. *Soft Matter, 7*(9), 4101–4110.

Vaz, W. L. C., Goodsaidzalduondo, F., & Jacobson, K. (1984). Lateral diffusion of lipids and proteins in bilayer-membranes. *FEBS Letters, 174*(2), 199–207.

Wawrezinieck, L., Rigneault, H., Marguet, D., & Lenne, P.-F. (2005). Fluorescence correlation spectroscopy diffusion laws to probe the submicron cell membrane organization. *Biophysical Journal, 89*(6), 4029–4042.

Weigel, A. V., Ragi, S., Reid, M. L., Chong, E. K., Tamkun, M. M., & Krapf, D. (2011). Obstructed diffusion propagator analysis for single-particle tracking. *Physical Review E, 85*(4), 041924.

Weigel, A. V., Simon, B., Tamkun, M. M., & Krapf, D. (2011). Ergodic and nonergodic processes coexist in the plasma membrane as observed by single-molecule tracking. *Proceedings of the National Academy of Sciences of the United States of America, 108*(16), 6438–6443.

Weigel, A. V., Tamkun, M. M., & Krapf, D. (2013). Quantifying the dynamic interactions between a clathrin-coated pit and cargo molecules. *Proceedings of the National Academy of Sciences of the United States of America, 110*(48), E4591–E4600.

Weiss, M. (2013). Single-particle tracking data reveal anticorrelated fractional Brownian motion in crowded fluids. *Physical Review E, 88*(1), 010101.

Weiss, M., Guigas, G., & Kalla, C. (2007). Probing the nanoscale viscoelasticity of intracellular fluids in living cells. *Biophysical Journal, 93*(1), 316–323.

Weiss, M., Hashimoto, H., & Nilsson, T. (2003). Anomalous protein diffusion in living cells as seen by fluorescence correlation spectroscopy. *Biophysical Journal, 84*(6), 4043–4052.

Winder, S. J., & Ayscough, K. R. (2005). Actin-binding proteins. *Journal of Cell Science, 118*(4), 651–654.

Wu, M. M., Covington, E. D., & Lewis, R. S. (2014). Single-molecule analysis of diffusion and trapping of STIM1 and Orai1 at ER-plasma membrane junctions. *Molecular Biology of the Cell, 25*(22), 3672–3685.